Chemical warfare agents and their interactions with solid surfaces

Agnieszka Anna Gorzkowska-Sobas

Norwegian Defence Research Establishment (FFI)

1 March 2013

Keywords

Kjemiske stridsmidler

Kjemiske stridsmidler – nedbrytning

Overflatekjemi

Overflatebehandling

Approved by

Stig Rune Sellevåg	Project Manager
Jan Ivar Botnan	Director

English summary

This literature study describes the interactions of chemical warfare agents (CWA) with materials. The materials of interest are various construction materials (concrete, plastics) and different types of surface finishing which are commonly used in urban environment or during military operations. Physical mechanisms (absorption, permeability) as well as chemical reactions (degradation) occurring on the surfaces are described, and their influence on the CWA persistency is given. It was found that degradation occurs mainly on basic surfaces, and the toxicity of the reaction products is affected by the experimental conditions and the condition of the surface. The principles behind new technologies emerging in the field of surface treatment have been included: the so-called omniphobic surfaces, able to repel any kind of liquid and the strippable coatings – paint which can be easily removed if it becomes contaminated.

Sammendrag

Det er gjennomført en litteraturstudie av kjemiske stridsmidlers vekselvirkninger med materialer. Materialene er hovedsakelig ulike konstruksjonsmaterialer (betong, plast) eller forskjellige typer av overflatebehandling som vanligvis brukes i et bymiljø eller i militært materiell. Fysiske mekanismer (absorpsjon, gjennomtrengelighet) og kjemiske reaksjoner (nedbrytning) har blitt gjennomgått sammen med deres innflytelse på vedvarenhet av kjemiske stridsmidler. Det ble funnet at nedbrytning av kjemiske stridsmidler skjer på overflater med basiske evner, mens giftigheten til nedbrytningsprodukter varierer avhengig av eksperimentelle betingelser og tilstanden til overflaten. Det beskrives også prinsipper til nye teknologier innen overflatebehandling: de såkalte omnifobiske overflater som avstøter alle typer av væsker og "strippable coatings" - maling som kan lett fjernes etter at den har blitt kontaminert.

Contents

1   Introduction

Even though the development, production and use of the chemical warfare agents (CWA) were banned by the Chemical Weapons Convention from 1993, the agreement was not ratified by all the world countries. Stockpiles of CWA still exist in several countries since the destruction of such weapons is a high-priced and technologically challenging process. For those reasons, even though their production was discontinued decades ago, the CWA still pose a threat to the military and civilians. In particular, in the big cities where the population and housing densities are high, a terroristic attack involving CWA would yield great number of casualties and vast economic loss.

The purpose of this report is to provide an overview of possible interactions between CWA and surfaces of various materials, including those commonly present in the urban environment. Large number of available reports focuses on CWA fate in case of spreading in the natural outdoor environment (water pools, areas covered by plants) and their influence over materiel. Concurrently, considerably less research on civilian materials has been published in the open literature. In this report different aspects of CWA interactions ranging from physical (adsorption, permeation, wetting) to chemical (corrosion, degradation) with various surfaces and their influence on CWA's persistence and fate have been presented. The importance of proper understanding of the phenomena associated with CWA-material surface interactions, as well as nature of the interface between them cannot be overlooked. It is crucial for their decontamination or disposal and also for finding efficient methods of preventing the contamination or minimizing the consequences of CWA-involving events.

The outcomes of the scientific investigations in this area resulted in rise of new technologies, such as slippery liquid-infused porous surfaces SLIPS [1] and self-decontaminating paints [2]. In particular, SLIPS seem to be a major technological advance in the field of anti-freezing and omniphobic coatings and is of special interest for the military forces as well as for civilian industry. Description of SLIPS and the principle of operation are to be found in Chapter 3. In addition, some construction materials show chemical activity towards CWA and accelerate their degradation rate. The general classification of different materials together with their permeability and absorption data were given in Chapter 4. Materials of interest include concrete, various plastics and rubbers, paints and coatings. However the exact mechanisms of degradation reactions on the materials surfaces and in the bulk depend on many variables, some of them often beyond human control (e.g. weather conditions). In some cases degradation processes is only partially successful, as the reactions yield dangerous products of relatively high toxicity. For this reason the awareness of possible consequences of contamination is vital to determine the risks and eliminate hazards related to remediation of the civilian areas or decontamination during military operations.

2 Classification of chemical warfare agents

Chemical warfare agents (CWA) are non-explosive chemical compounds used to kill, injure or incapacitate humans. CWA can be classified according to their physiological actions on a human body. Different classes of CWA are given below together with chosen representatives and their relevant physicochemical properties [3, 4].

2.1 Choking agents

Choking agents are chemicals that cause irritation of the respiratory track and attack lung tissue, causing pulmonary edema. In extreme cases membranes swell, lungs become filled with liquid and a victim suffocates due to lack of oxygen.

Table 2.1   Principal choking agents and their physicochemical properties.

Common name and designation	Chlorine CL	Phosgene CG	Diphosgene DP
Chemical formula	Cl_2	$COCl_2$	$C_2Cl_4O_2$
Physical state at 20°C	Gas	Gas	Liquid
Boiling point [°C]	-34	7.8	127
Vapor pressure [mm Hg]	5168 at 21 °C	1400 at 25 °C	4,41 at 20 °C
Volatility [mg/m³]	$2.19x10^7$ at 25 °C	$7.46x10^6$ at 25 °C	$4.8x10^4$ at 20 °C
Vapor density (air=1)	2.5	3.4	6.8
Persistency	Non-persistent	Non-persistent	Non-persistent

2.2 Nerve agents

Nerve agents are organophosphate esther derivatives of phosphoric acid. They act as acetylcholinesterase inhibitors, which is an enzyme degrading the neurotransmitter acetylcholine. In brief, acetylcholine enables a communication between the nerve cells and the muscle cells, which is responsible for e.g. muscle contraction. As a result the acetylcholine accumulates disrupting normal functioning of muscles and nerves. Toxicity of nerve agents is much higher than other CWA. Two groups of nerve agents are distinguished due to their chemical composition: G-agents (fluorine- or cyanide-containing organophosphates) and V-agents (sulfur-containing organophosphates).

Table 2.1   Principal nerve agents and their physicochemical properties.

Common name and designation	Sarin GB	Tabun GA	Soman GD	Cyclosarin GF	VX
Chemical formula	$C_4H_{10}FO_2P$	$C_5H_{11}N_2O_2P$	$C_7H_{16}FO_2P$	$C_7H_{14}FO_2P$	$C_{11}H_{26}NO_2PS$
Physical state at 20 °C	Liquid				
Boiling point [°C]	150	248	198	228	292
Vapor pressure [mm Hg]	2.48 at 25 °C	0.057 at 25 °C	0.4 at 25 °C	0.0927 at 25 °C	0.0009 at 25 °C
Volatility [mg/m³]	1.8×10^4 at 25 °C	497 at 25 °C	4×10^3 at 25 °C	898 at 25 °C	10 at 25 °C
Vapor density (air=1)	4.8	5.6	6.3	6.2	9.2
Persistency	Non-persistent			Persistent	

2.3   Blistering (vesicant) agents

These agents impose damage on every tissue they come in contact with, blistering skin, damaging the respiratory tract when inhaled and causing vomiting and diarrhea when absorbed.

Table 2.2   Principal blistering agents and their physicochemical properties.

Common name and designation	Sulfur mustard HD	Nitrogen mustard HN-1	Nitrogen mustard HN-2	Nitrogen mustard HN-3	Lewisite L	Phosgene oximine CX
Chemical formula	$C_4H_8C_{l2}S$	$C_6H_{13}Cl_2N$	$C_5H_{11}Cl_2N$	$C_6H_{12}Cl_3N$	$C_2H_2AsCl_3$	$CHCl_2NO$
Physical state at 20 °C	Liquid					Solid below 39°C
Boiling point [°C]	218*	192*	177*	257*	196*	129*
Vapor pressure [mm Hg]	10 at 25 °C	24.4 at 25 °C	0.4 at 25 °C	0.011 at 25 °C	3.46 at 25 °C	11.2 at 25 °C
Volatility [mg/m³]	906 at 25 °C	2230 at 25 °C	3490 at 25 °C	120 at 25 °C	3860 at 25 °C	1800 at 20 °C 7600 at 40 °C
Vapor density (air=1)	5.5	5.9	5.4	7.1	7.1	3.9
Persistency	Persistent					Non-persistent

* decomposes below boiling point

2.4 Blood agents

These agents block the transfer of oxygen from blood to the cells of the body by poisoning the enzyme cytochrome oxidase, which results in asphyxiation.

Table 2.3   Principal blood agents and their physicochemical properties.

Common name and designation	Hydrogen cyanide AC	Cyanogen Chloride CK	Arsine SA
Chemical formula	HCN	CNCl	AsH_3
Physical state at 20 °C	Liquid	Gas	Gas
Boiling point [°C]	25.5	12.8	-62.5
Vapor pressure [mm Hg]	760 at 25 °C	1000 at 25 °C	$11.1x10^3$ at 20 °C
Volatility [mg/m³]	$1.1x10^6$ at 25 °C	$2.6x10^6$ at 20 °C	$31x10^6$ at 20 °C
Vapor density (air=1)	0.99	2.1	2.7
Persistency	Non-persistent		

2.5 Vomiting agents

Vomiting agents irritate the upper respiratory tract and eyes, causing sneezing, coughing, nausea, tearing and general bodily discomfort. The agents listed below are solids that vaporize when heated and then condense to form aerosols.

Table 2.4   Principal vomiting agents and their physicochemical properties.

Common name and designation	Adamsite DM	Diphenylchloroarsine DA	Diphenylcyanoarsine DC
Chemical formula	$C_{12}H_9AsClN$	$C_{12}H_{10}AsCl$	$C_{13}H_{10}AsN$
Physical state at 20 °C	Solid		
Vapor pressure [mm Hg]	$2x10^{-13}$ at 20 °C	$3.6x10^{-3}$ at 45 °C	$2x10^{-4}$ at 20 °C
Boiling point [°C]	410*	333*	350*
Melting point [°C]	195	41 – 44.5	31.5 – 35
Vapor density (air=1)	negligible	9.15	No data available
Volatility [mg/m^3]	$26x10^3 – 120x10^3$ at 20 °C	48 at 45 °C	2.8 at 20 °C
Persistency	Aerosol form: short, solid state: long		

* decomposes upon boiling

2.6   Persistency

One of the most important characteristics of CWAs is their persistency – "a period of time during which the agent retains its toxicity in the air or on the ground" [5]. CWA is considered persistent if it remains able to cause casualties for more than 24 hr to several days after it was released, whereas a non-persistent one dissipates or loses ability to cause casualties after 10 to 15 minutes [4]. Therefore the persistent CWA, apart from casualties, will also cause a long-lasting contamination of the terrain and materiel, hampering their use. However, estimating the exact persistency is very complex, since it depends on many factors, such as physical and chemical characteristics of the agents, the conditions of the environment: weather (temperature, atmospheric drop, humidity and sunlight), terrain topography outdoors, ventilation system and architecture indoors; state of the affected surfaces and the way of dissemination. Weather in particular can affect both the duration and the likelihood of a CWA-involving episode, since the effectiveness of the CWAs depend on the atmospheric conditions [6]. It has been shown that the low temperatures may significantly increase the persistency of an agent (Figure 2.1) [7]. For example, the GB nerve agent which is considered as non-persistent may remain a transfer hazard for up to 30 days in cold climates [8, 9]. It was also shown that in winter conditions after 4 weeks the nerve gases could be still detected, and when the samples were covered by snowfall the recovery remained high [7, 9, 10].
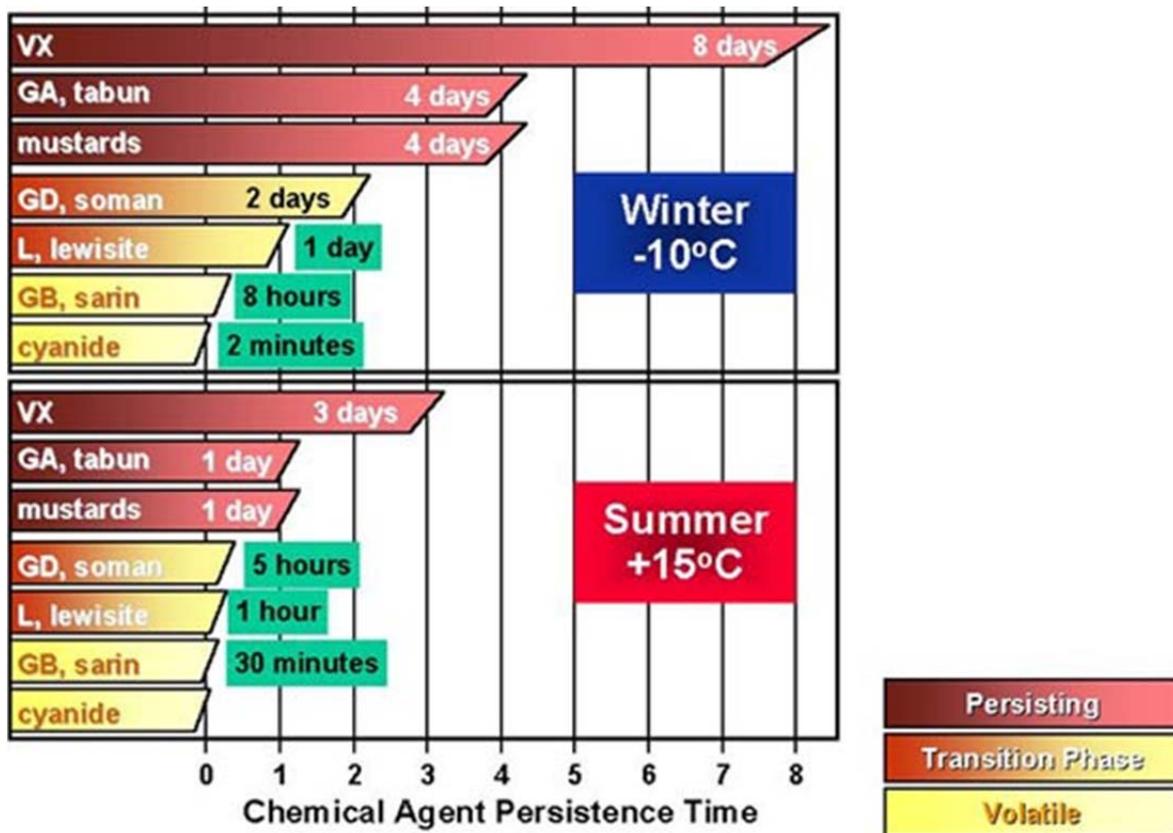
Figure 2.1   The approximate persistency of the chosen CWA under generalized winter and summer conditions [11].

Some of the physical and chemical properties of the CWA important for the persistency assessment are briefly described below.

- **Vapor pressure**

It is the pressure exerted by the vapor in equilibrium with its condensed phase (liquid or solid) at a given temperature. The vapor pressure increases with increasing temperature.

- **Boiling point**

Boiling is observed when the vapor pressure above the liquid is equal to the pressure of a gas above this liquid. The boiling point of water is 100 °C when the atmospheric pressure is 1 atm. The lower is the boiling point (or the lower the surrounding pressure), the faster the evaporation rate and the lower persistency.

- **Volatility**

Volatility is the tendency of the condensed phase (solid) to vaporize. Volatility depends on the vapor pressure and the temperature. The lower volatility of the agent, the more time it will take to evaporate, and the higher will be their persistency. Volatility is given in milligrams of vapor per cubic meter.

One should note that knowing what amount of agent is present as vapor in the environment will not suffice to estimate the casualties caused by it. As can be seen from Table 2.1 VX is almost 2000 times less volatile than GB, however it has higher toxicity and therefore a much smaller amount of vapor is needed to achieve the same lethality. The toxicity of an agent is usually given as a **Median Lethal Dosage LD50** for liquid agents – the amount lethal to 50% of exposed unprotected individuals, and **Median Lethal Dosage LCt50** for a vapor or aerosol – the amount lethal to 50% of exposed unprotected individuals for defined minute volume, MV and exposure duration. **MV** is the volume of air exchanged in one minute by a person.

Table 2.5   Comparative volatilities and lethal doses for chosen chemical warfare agents [3]

Agent	Volatility [mg/m^3] at 25°C	Lethal dose (respiratory) [mg min/m^3]
Hydrogen cyanide (AC)	1 000 000	2000
Sarin (GB)	22 000	70-100
Soman (GD)	3 900	70-400
Sulfur Mustard (HD)	900	1000-1500
Tabun (GA)	610	135-140
VX	10	30

- **Vapor density**

The ratio of the weight of a given volume of the gas phase and the same volume of another gas measured under the same conditions of pressure and temperature. Most often air is the reference gas – if the vapor density of an agent is more than 1, the agent will tend to settle on the ground.

- **Ability to penetrate the ground and various materials.**

Fast absorption of an agent in the soil or other materials on the ground decreases the contamination rate and CWA combat efficiency [5]. This however makes decontamination process difficult, if not impossible. In addition, the toxic vapors can be released long time after the event, causing further contamination.

- **Reactivity**

The persistency will also be dependent on the chemical properties of the CWA, such as its reactivity towards different substances in the environment. If left in the natural environment they will eventually decay (weathering). The main reactions are [11]:

- hydrolysis with water in the environment
- oxidation by atmospheric oxygen
- photochemical reactions with sunlight
- thermochemical decomposition
- other reactions with compounds present in the environment (coverings, vegetation, surfaces)

Even though passive decontamination through weathering does not require any human intervention and is economically beneficial, it is a long-lasting process and its efficiency largely depends on the weather conditions [12]. Hydrolysis is perhaps the most important of the aforementioned processes, since water or its vapor is ubiquitous in both outdoor and indoor environments. During hydrolysis chemical bond in a molecule becomes cleaved and water molecule is added to both parts as hydrogen cation and hydroxide anion. As a result, different chemical compounds are formed, some of them being harmless, other nearly as toxic as the original. Moreover, water is adsorbed on many surfaces and its presence affects the interaction of CWAs with those surfaces. The following section gives details on the hydrolysis reactions and their products of the most persistent CWAs.

2.6.1   Hydrolysis of sulfur mustard

Sulfur mustard (HD) is relatively stable, and its persistency is particularly high in the dry or cold environments. HD rapidly reacts with water, but its solubility is very limited, and it can actually survive under water or in extremely humid environment for years [13]. HD hydrolysis is relatively complex, and the final products formation will depend on the temperature and the amount of water available [14, 15]. Some of the products of HD hydrolysis reactions are as potent vesicants as the parent compound. It was reported that the amount of water present in the environment, mechanical action (stirring), and presence of other chemicals affecting mustard's solubility (acetone) will affect the rate of hydrolysis and its products [15].

Basic scheme of HD hydrolysis is shown in Figure 2.2. Dissolved HD is first converted to sulfonium ion and then reacts with water molecule forming mustard chlorohydrin (hemisulfur mustard) and HCl. Next a thiodiglycol (TDG) product is formed.
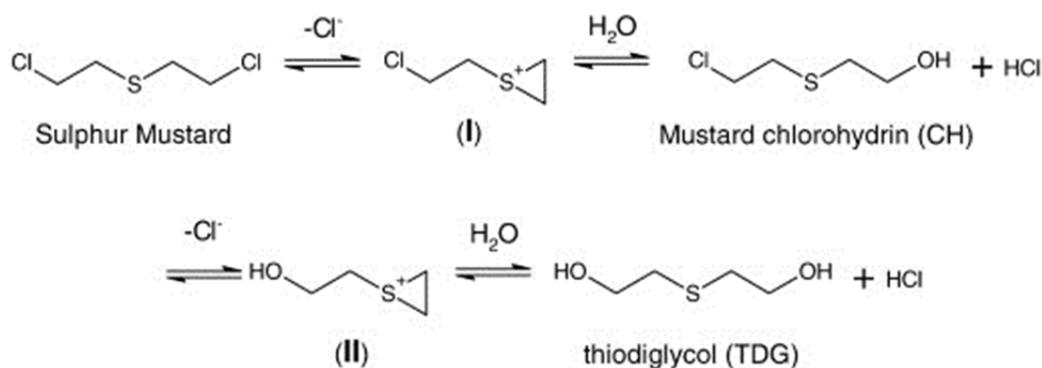

Figure 2.2   Hydrolysis of sulfur mustard (HD)[11]

The internal displacement of intermediate product (II) can yield 1,4-thioxane (Figure 2.3). TDG to 1,4-thiooxane ratio is about 4:1[11].
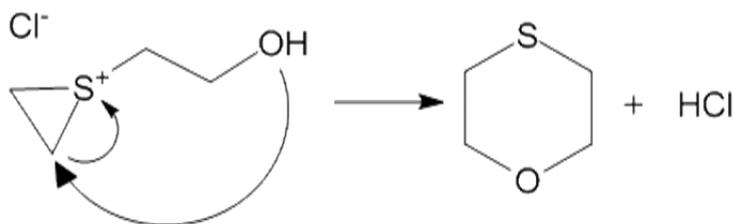
Figure 2.3   1,4-thioxane formation upon HD hydrolysis [11].

One can see that during HD hydrolysis toxic TDG and CH are formed, as well as highly corrosive hydrochloric acid HCl.

Munro et al. described the following pathway of HD hydrolysis, including the reactions among intermediate products of hydrolysis (Figure 2.4) [14]. In the environment where the water is scarce, the reactants, products and intermediates of hydrolysis will react with each other, forming various sulfonium aggregates.
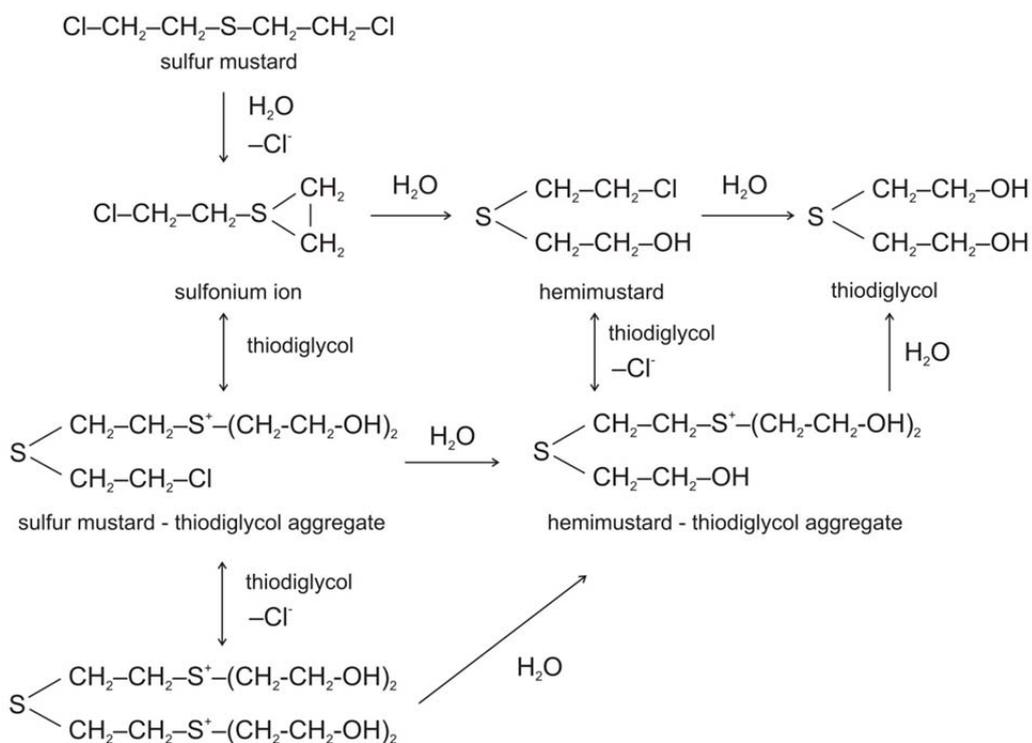

Figure 2.4   Primary hydrolysis pathways of mustard (HD) [14].

Other reactions which are likely to occur between the hydrolysis products and sulfonium ions are shown in Figure 2.5. Possible reaction products include H-2TG (Sulfonium, (thiodi-2,1-ethanediyl)bis[bis(2-hydroxyethyl)-), CH-TG (Sulfonium, (thiodi-2,1-ethanediyl)bis[bis(2-

hydroxyethyl)-) and H-TG (Sulfonium). The toxicity of sulfonium species is probably similar to that of HD, and their persistency and water solubility not well documented. Formation of those products is believed to be responsible for high persistency of HD in quiescent water, as they form a stable layer around the primary droplet, preventing bulk mustard from further hydrolysis reactions [11, 15]. In addition, hydrolysis will proceed differently in sea water [13], and in alkaline (pH>7) or acidic (pH<7) solutions. More detailed information about possible degradation products of HD can be found in references [13, 14].
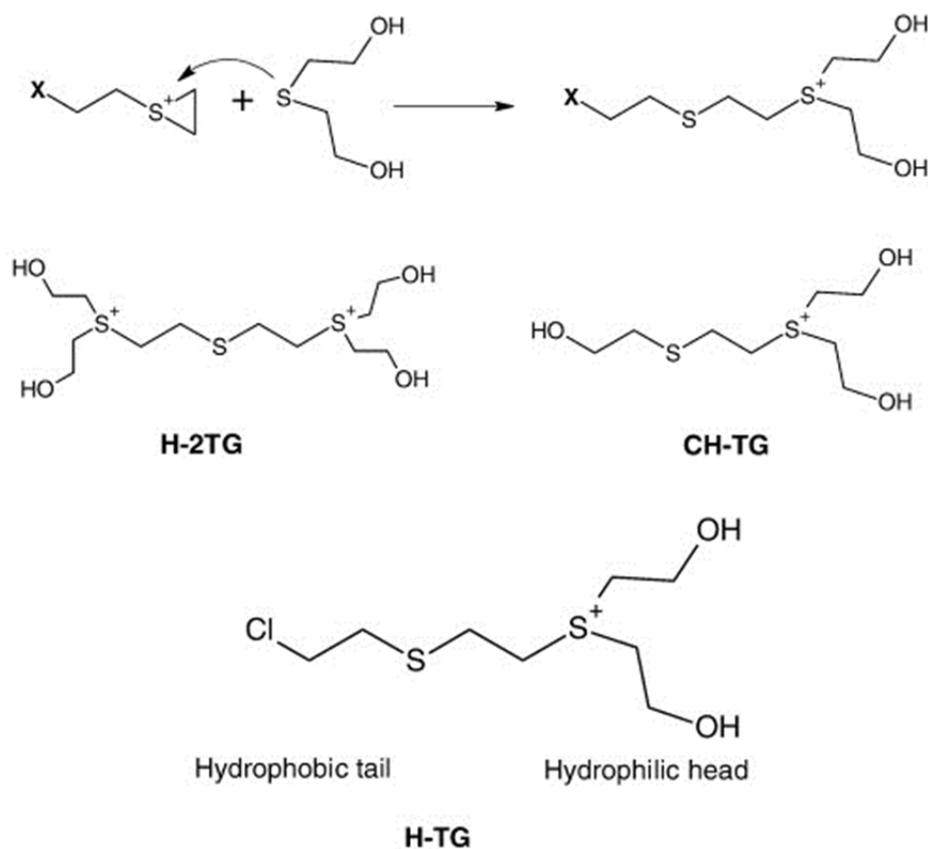

Figure 2.5   Reaction between a sulfonium intermediate and TDG and other possible products (sulfonium ions): H-2TG, CH-TG and H-TG [15].

2.6.2   Hydrolysis of VX

VX is relatively resistant to hydrolysis, with half-life in pure water reported to be 60 hours and hydrolysis mechanism and products forming depend on pH of the environment [4]. Possible mechanisms of VX hydrolysis are shown in Figure 2.6.
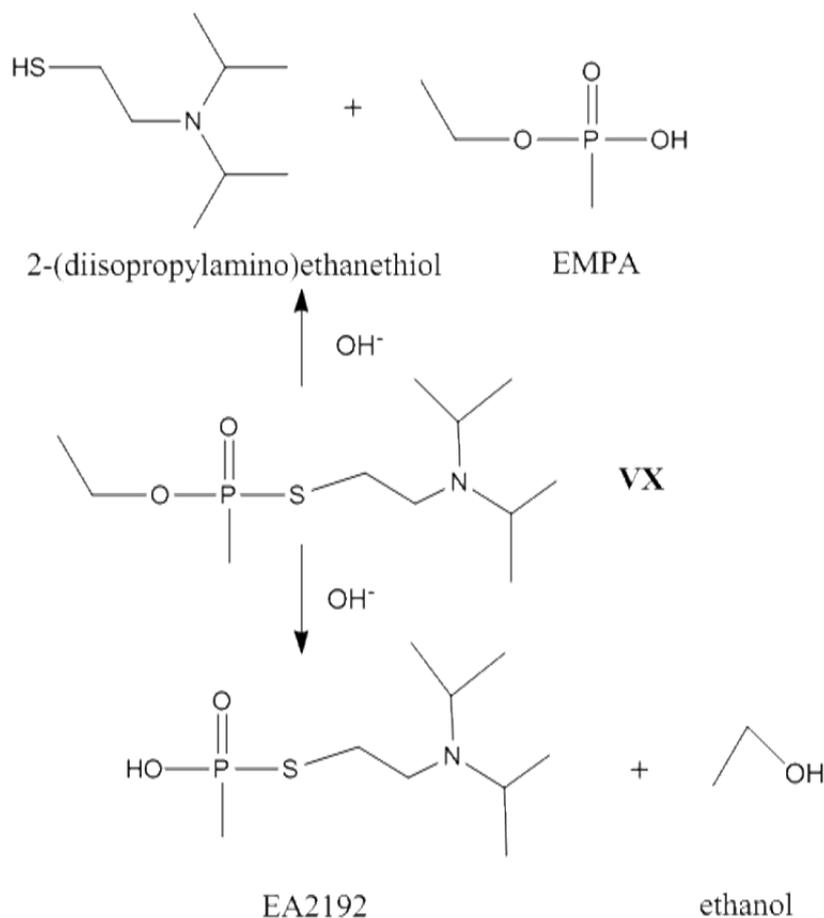
Figure 2.6   Hydrolysis reaction for VX [16]

In the first case a 2-(diisopropylamino)ethanethiol (DESH) and ethyl ester of methylphosphonic acid (EMPA) are formed via P-S bond cleavage (Figure 2.7, scheme 2), whereas in the second S-(2-[diisopropylamino]ethyl) methylphosphonothiolate (EA-2192) and ethanol are formed via P-O bond cleavage (Figure 2.7, scheme 3) [17]. Whereas the toxicity of the first two compounds is low, EA-2192 is reported to be nearly as toxic as VX if administered intravenously [16]. In alkaline environments VX hydrolysis is nonselective, forming a mixture of those products, with approximately 22% of EA-2192 [18]. Hydrolysis in water was reported to be selective and yield EMPA [19]. According to another study in distilled water 42-50% of the product is formed due to P-O bond cleavage, 34-37% due to P-S bond cleavage and rest due to C-S bond cleavage (Figure 2.7, scheme 4); for pH<6.5 and pH>10 decomposition via P-S bond cleavage occurs [17]. For detailed information on VX hydrolysis one can also refer to references [20, 21].

Scheme 1
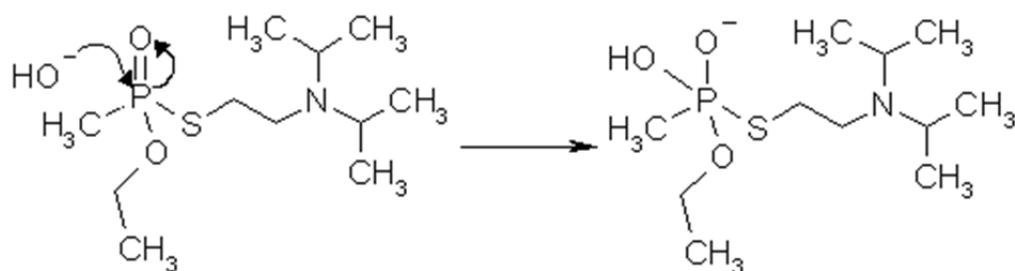
Scheme 2
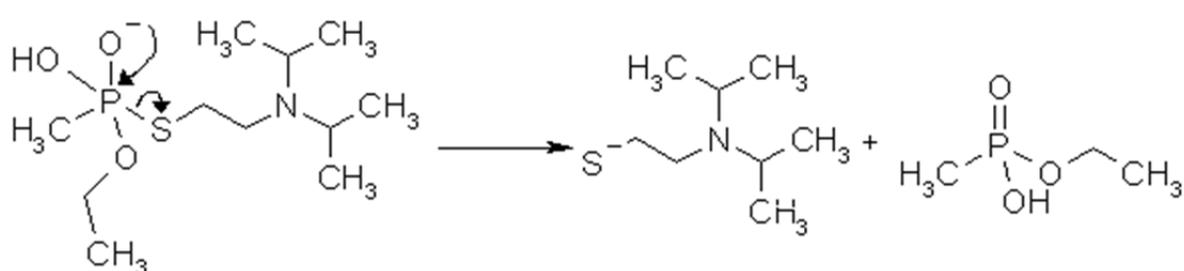
Scheme 3
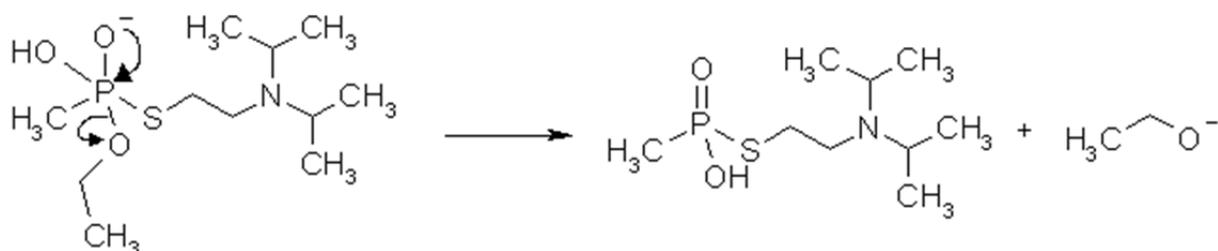
Scheme 4
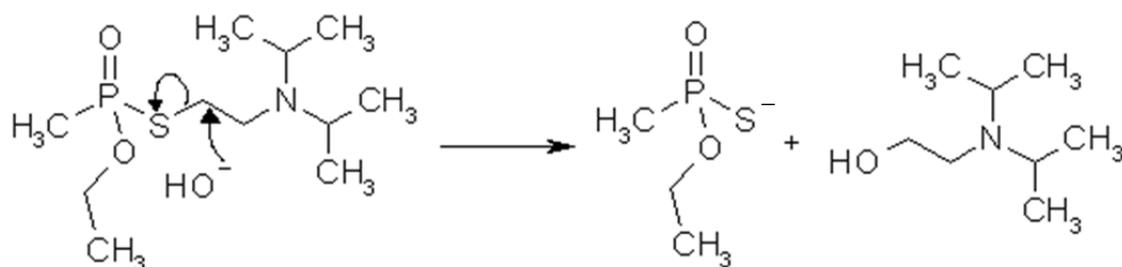
Figure 2.7   Schemes of VX decomposition. Scheme 1 shows a phosphorus intermediate
formation via nucleophilic attack of OH- on phosphorus atom. The intermediate
undergoes decomposition via P-S bond cleavage (scheme 2) or P-O bond cleavage
(scheme 3) yielding products of different toxicity. Scheme 4 shows mechanism of C-S
bond cleavage via displacement of thiophosphonate anion [17]

3 Mechanisms of surface contamination and physical interactions

CWAs can have different physical forms: solid, liquid or gaseous. Most liquids and solids can be prepared in forms of aerosol or smoke for rapid dispersion over a large area. After release a suspension of smaller droplets will form a primary cloud, which under favorable atmospheric conditions may spread over large distances. Large droplets will tend to remain at or close to the point of release, contaminating the surroundings. Depending on their volatility they may evaporate forming a secondary cloud [5, 22].

In case of surface contamination physical and chemical properties of CWA will influence the contact time and spreading mechanism over and into the contaminated surface. This in turn will affect the agent's persistency and the properties of the material. A substantial amount of work on the CWA's effects on materiel and outdoor environment has been published as a result of the military research. These reports focus mainly on the materials survivability, CWA effect on their functional properties (mechanical, electrical and chemical), and possibilities of decontamination. However, the data is often collected during tests under standardized laboratory conditions, which do not necessarily reflect realistic settings and therefore they are useful to evaluate the perseverance of contamination and the appropriate decontamination procedures only to a certain extent.

3.1 Gaseous CWA

The gaseous CWAs tend to spread relatively quickly and dissipate, especially outdoors, therefore their persistence is considered as low. However, the gaseous agents may become temporarily immobilized by means of physical adsorption and in some cases, chemical. In the first case, there is no chemical bond formed and CWA bind with the surface by means of weak van der Waals and electrostatic interaction. As a result the contact time is short and wind outdoors or sufficient ventilation indoors will remove the gas. The second occurs when the gaseous CWA reacts with the surface. An example here could be chlorine gas (Cl_2), which is highly reactive towards certain polymers and bare metal surfaces, and when in contact with water forms a highly corrosive HCl acid. It is also heavier than air and will therefore linger at the bottom of the contaminated area, making it more difficult to eliminate.

3.2 Solid CWA

CWAs in the solid state are mainly vomiting agents, and they are considered as highly persistent. When employed, the vapor is produced upon heating and then condensates forming an aerosol. Some of those agents are reported to be highly corrosive towards metals, especially when they contain impurities, which can make them difficult to handle and store [3].

Other kind of solid CWA are the so called dusty agents (toxic dust or dust-impregnated agents). They are produced when the liquid CWA, usually mustard gas (HD) or sarin (GB), is absorbed in a solid matrix, such as silica, from which the vapors are gradually released [4]. Their inhalation

toxicity is reported to be highly increased. Here, no other extra effects apart from the ones typical for the liquid or gaseous CWA can be expected.

3.3 Liquid CWA

Liquid CWA are among the most persistent agents and for this reason they are often subjects of research on CWA – materials interaction and decontamination. When a liquid CWA is employed it will rest on the surface in the form of splashes or droplets. The size (volume) and distribution of the droplets will largely depend on the way of employing the CWA. The droplets may then get absorbed, evaporate, undergo a chemical change (reaction with the surface or with the ambient, e.g. hydrolysis) or all the above, depending on the physicochemical properties of the agent and the material.

The following paragraphs include useful definitions needed to understand phenomena associated with liquids and a number of case studies for liquid CWA and materials interactions.

3.3.1 Liquids - theoretical background

Liquid as a state of matter falls between gases and solids. Typical behavior of liquids is similar to gases: they tend to flow and take the shape of the container, but unlike gases they have a distinct surface and their density is fairly constant.

Atoms or molecules on the surface are not equally surrounded by their neighbours, unlike those in the bulk of the solid or liquid, and some of their bonds are unsaturated. As a result, their energy is higher than the atoms or molecules in the bulk. This excess energy is called surface energy. Thermodynamically the surface energy can be understood as a work needed to create a unit area of a new surface:

$$dw = \gamma dA \qquad\qquad (3.1)$$

where *dw* is the work done to create an infinitesimal change in a surface area *dA*. The proportionality constant γ is called the surface tension (J/m^2) [23]. High surface energy ranging between 100-5000 mJ/m^2 is observed in case of solids with metallic, covalent or ionic bonding e.g. metals, metal oxides, glass; polymers and plastics have usually surface energies below 50 mJ/m^2. In general, the higher the melting point and the greater the hardness the higher the surface energy of a solid [24].

3.3.2 Surface tension and droplet formation

In case of liquids their surface energy is numerically equal to surface tension γ[1] [25, 26]. Surface tension results from the forces of cohesion between the molecules of the liquid. The molecules in

---

[1] There is ongoing discussion what is the relation between "surface tension" and "surface energy" in case of unstrained solids. Originally this was given by Shuttleworth's equation [25] however it was recently shown by Makkonen [26] that surface energy as defined by Shuttleworth can be reduced to mechanical definition of surface tension. For more information one can refer to original works [25] and [26].

the bulk are surrounded by the neighboring molecules, so that the net force experienced by each of them is zero, but at the phase boundary the molecules are not surrounded from all sides and are pulled inwards. As a result the surface of the liquid contracts to the smallest possible surface area. This phenomenon is responsible for the liquid droplets shape, since for a given volume of a liquid a shape with minimum surface-to-volume ratio is a smooth sphere. Schematically the forces of attraction among the molecules in a liquid are shown in Figure 3.1 .
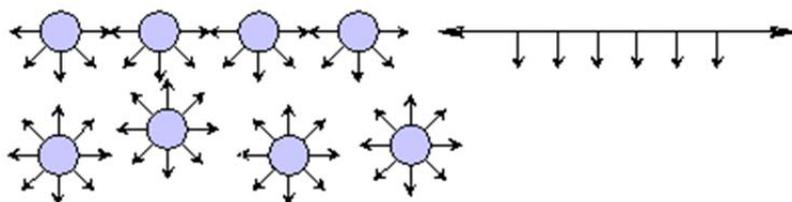

Figure 3.1   Interactions between the molecules in the bulk and close to the surface of a liquid. Forces acting on the molecules on the surface are not in equilibrium, and the molecules are pulled inwards.

The concept of surface tension is helpful in explaining why objects or liquids of greater density than water are able to sit on its surface (Figure 3.2), provided it is sufficiently immobile. For example HD was reported to persist on water surface for several days [27]. HD is denser than water, but HD in form of droplets or film may still linger on quiescent water surface due to the difference in surface tension of those liquids (γ_{HD} is 42.5 mN/m, whereas γ_{water} is 78.2 mN/m [4]). Since HD has very limited solubility, such behavior also contributes to prolonged persistency.

Figure 3.2   A metal paper clip is held on water surface due to its high surface tension [28]

3.3.3   Capillary action

One of the consequences of a surface tension is a capillary action, observed when a narrow tube (a capillary) is inserted into a liquid. For instance, if a glass tube is immersed in water, the liquid creeps up the walls of the tube due to forces of adhesion (interaction between water molecules and surface of the glass, Figure 3.3). As a result the surface of the liquid (so called "meniscus")

becomes curved [23]. Meniscus curvature will depend on the balance between forces of adhesion between the liquid and the capillary walls, and the forces of cohesion (interaction between the liquid molecules). If the forces of adhesion are weaker than forces of cohesion within the liquid, the liquid retracts from the glass and its surface is concave; conversely, when the forces of cohesion are weaker, meniscus will be convex.

The pressure difference across the curved liquid/air interface inside the capillary is given by the Young-Laplace equation:

$$\Delta p_c = \frac{2\gamma cos\theta}{r_{cap}} \qquad (3.2)$$

where γ is the surface tension, θ is the contact angle, r_{cap} is the capillary radius. In terms of contact angle one can see that if the wettability is high (low contact angle), the liquid inside the capillary will form a concave meniscus and the capillary pressure will be negative, resulting in the liquid being pulled into the capillary; at a high contact angle the meniscus will be convex, and the liquid will have to overcome the capillary pressure to propagate into the capillary.
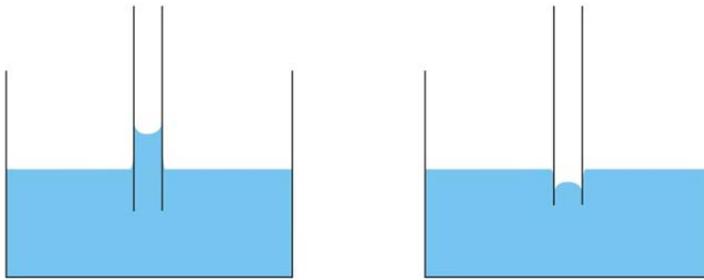

Figure 3.3   The capillary action when forces of cohesion are greater (left side) and smaller
(right side) than the forces of cohesion within the liquid.

At equilibrium the forces of adhesion are equal to the weight of a liquid in a capillary. Hydrostatic pressure p exerted by a column of liquid of mass density ρ and height *h* is given by the equation:

$$p = \rho gh \qquad (3.3)$$

where *g* is the standard acceleration of gravity.

3.3.4   Contact angle and wetting

When a droplet is placed on a surface, it will spread until equilibrium spread diameter is reached. For a drop of liquid resting on a solid surface and surrounded by an ambient atmosphere the equilibrium is attained by the force balance at the boundary of all the three phases (Figure 3.4):
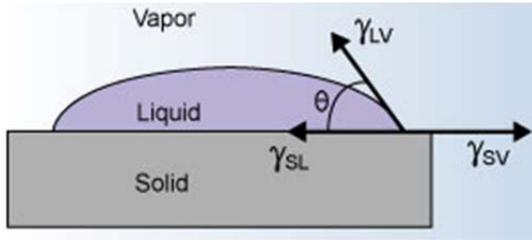
Figure 3.4   Forces exerted on a droplet of liquid resting on a solid and surrounded by ambient gas.

This equilibrium is described by Young's equation:

$$\gamma_{sv} = \gamma_{sl} + \gamma_{lv}cos\theta_c \qquad (3.4)$$

where γ_{sv}, γ_{sl} and $\gamma_{l,v}$ are solid-vapor, solid-liquid and liquid-vapor surface tensions, respectively, and θ is the contact angle. θ can be measured experimentally and characterizes the wettability of a surface. Work of adhesion of liquid to solid per unit area of contact is given by the following equation [23]:

$$w_{ad} = \gamma_{sv} + \gamma_{lv} - \gamma_{sl} \qquad (3.5)$$

Combining equations (4) and (5) we have:

$$cos\theta_c = \frac{w_{ad}}{\gamma_{lv}} - 1 \qquad (3.6)$$

Contact angle is used as a quantitative measure of wettability, i.e. the ability of a liquid to maintain contact with a solid surface, and its value is independent on the droplet volume. Surfaces exhibiting contact angles much higher than 90° are called "hydrophobic" (from Greek "hydro" – water, and "phobos" – fear), since they seem to repel water. Conversely, surfaces where contact angle is close to 0 are "hydrophilic" (Greek "philia" – love) [29].
Figure 3.5 shows different wetting conditions and the corresponding contact angle.
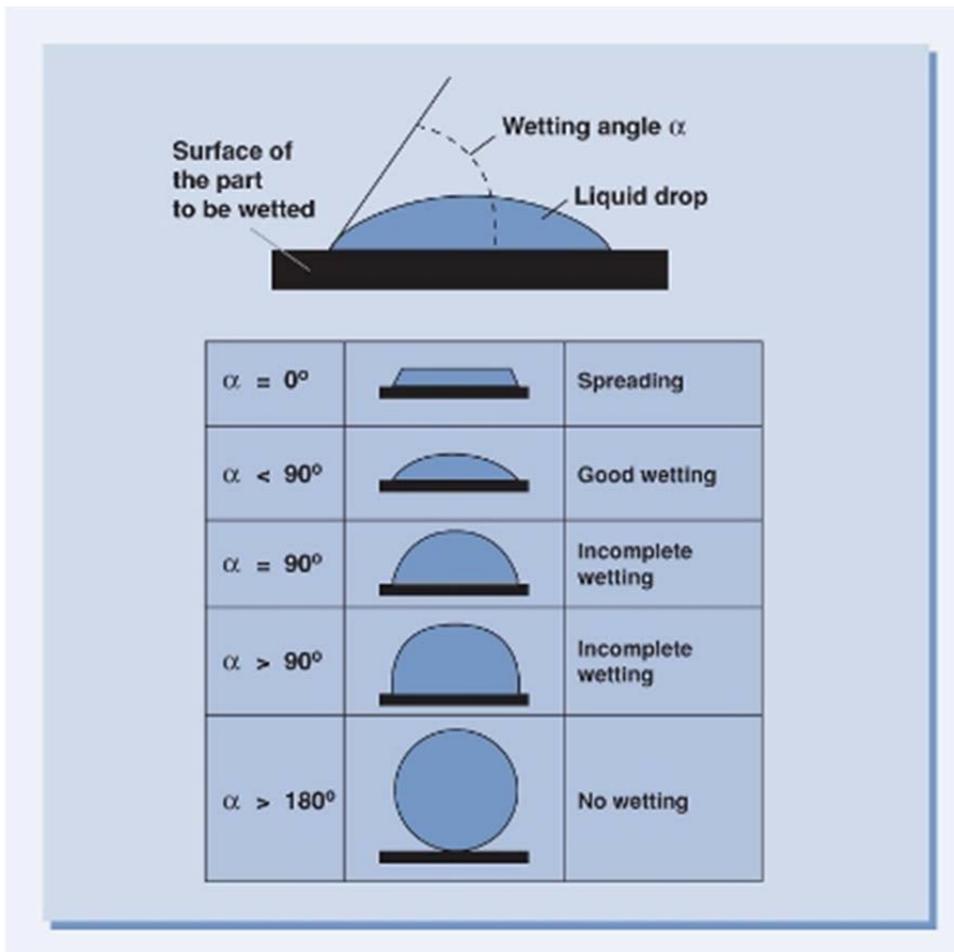
Figure 3.5   Wetting characteristics of a liquid and the corresponding contact angle [30]

According to equation (6) good wetting (θ_c between 0 and 90°) is achieved when $w_{ad} > 2\gamma_{lg}$, and the liquid does not wet the surface ($\theta_c > 90°$) when $w_{ad} < \gamma_{lg}$. In other words, a contact angle value comes from the balance between forces of cohesion between molecules of a liquid and forces of adhesion between the molecules of a liquid and a surface.

It should be noted that these considerations are mostly valid for flat and smooth surfaces of rigid solids. In reality surfaces exhibit certain roughness, tilting angle or curvature. For a droplet which is changing its volume or is placed on a tilted surface, two contact angles are observed: receding and advancing contact angles (Figure 3.6). This can be attributed to more than one thermodynamically stable contact angle achievable for a non-ideal solid. Difference between these two angles is called contact angle hysteresis.
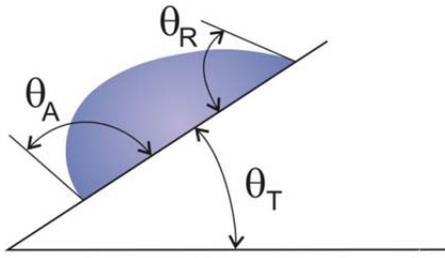
Figure 3.6   Advancing (θ_A) and receding (θ_R) contact angles for a droplet on a tilted surface (θ_T – tilt angle).

Wetting on rough surfaces can be described by Wenzel model, where the spaces between solid steps are filled with liquid [31] (Figure 3.7).
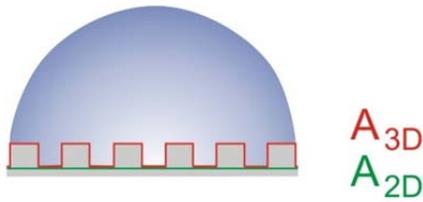

Figure 3.7   Wenzel model of wetting – complete wetting of the rough surface by the liquid droplet.

In such a case, the wetting angle is described by the equation:

$$cos\theta_a = rcos\theta \tag{3.7}$$

where θ_a is the apparent contact angle, θ is the equilibrium contact angle on a flat surface, is a ratio between real (A_{3D}) and projected (A_{2D}) area of the sample. When the surface is heterogeneous, or when the cavities are filled with air so that the droplet rests on a composite consisting of air and solid (Figure 3.8), wetting is described by Cassie-Baxter model [32]. The contact angle in such a case is given by the equation:

$$cos\theta_a = f_1 cos\theta_1 + f_2 cos\theta_2 \tag{3.8}$$

where f_1 and f_2 are area fractions of material 1 and 2, θ_1 and θ_2 contact angles for pure materials 1 and 2, respectively.
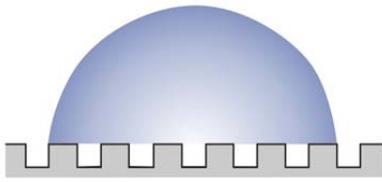
Figure 3.8   Cassie model of wetting, where a droplet rests on a rough surface with air pockets trapped between surface features.

Surface roughness can enhance hydrophilic (hydrophobic) properties, leading to super-hydrophilic or super-hydrophobic behavior. The most known phenomenon is the "lotus-leaf" effect by which certain plants can repel water entirely from their leaves owing to their nanostructured surface. Rough surface of a leaf contains tiny cavities in which air is trapped, forming pockets between the surface and the liquid. As a result the contact area is minimized and water does not adhere to the surface (Figure 3.9). Similar effects are also achievable on micro or nanostructured solids using photolithography, plasma or laser irradiation [33]. It should be noted that this behavior can be expected on a surface which is already hydrophobic, whereas in case of hydrophilic surface, a super-hydrophilic behavior can be expected. Furthermore, if enough pressure is applied to the liquid characterized by Cassie-Baxter model of wetting, it will eventually transform into Wenzel model and the surface will lose its hydrophobic properties.
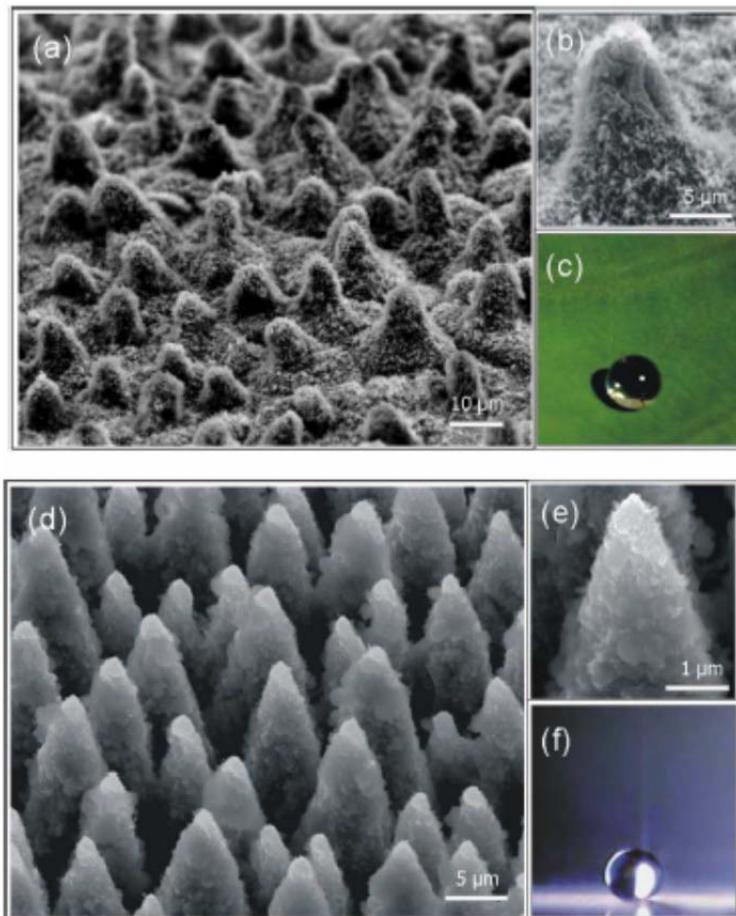
Figure 3.9   Scanning Electron Microscopy images and photographs of a lotus leaf (top) and silicon structure (bottom) showing the same superhydrophobic properties towards water droplet [33].

3.3.5   Hydrophobic and hydrophilic surfaces and their effect on sarin (GB) degradation

On atomic scale hydrophobic or hydrophilic properties of materials are a consequence of the specific structure of water molecule, which has linear distribution of electric charge and can be represented as an electric dipole (Figure 3.10 a) [29]. As a result it can interact electrostatically with other dipole-like (polar) molecules forming so-called hydrogen bonds (Figure 3.10 b). A hydrogen bond has a considerable strength of 10-40 kJ/mol and shows tendency to directionality and linearity. These bonds can also form during water interaction with solid surface. Characteristic feature of solid surface is the presence of certain charge due to unsaturated bonds. In addition, certain atoms or groups of atoms readily form hydrogen bonds with water molecules. In the presence of such surface water molecules will arrange themselves so that their charge has opposite sign to the charge of the surface [29]. Such surfaces will be hydrophilic. On the contrary, if material is non-polar and cannot form hydrogen bonds, the water molecules will arrange in such way that the number of unused hydrogen bonds is minimal (hydrophobic surface).
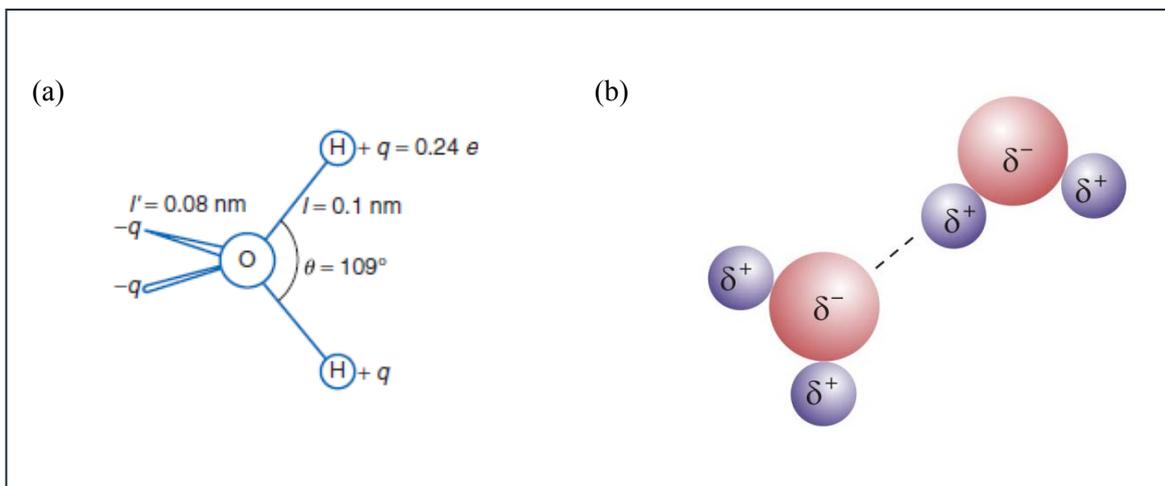
Figure 3.10 Sketch of water molecule with partial charges marked (negative on oxygen atom, positive on hydrogen atoms) [25]; (b) the schematic representation of hydrogen bond formation between polar molecules of water.

Hydrophobic or hydrophilic properties can affect the reactions occurring on or in the vicinity of the surface. For instance, surprisingly high values of the contact angle were observed for esters wetting the glass surface, although full wetting was expected [24]. It was suggested that the surface was hydrated prior to measurement, and the water molecules adsorbed on hydrophilic surface of glass were highly effective in causing hydrolysis of esters due to their orientation. As a result, a monolayer of hydrolysis products was formed on the surface, and the resulting contact angle was due to hydrophobic nature of this monolayer towards the droplet of ester.

Kuo et al. investigated the effect of surface hydrophilic and hydrophobic properties on sarin (GB) degradation in water by means of first-principles molecular dynamics simulations [34]. Three different scenarios of GB hydrolysis were considered, where a GB molecule was surrounded by water in the bulk, in vicinity of hydrophilic (glass slab or amorphous silica) and hydrophobic surface (butane). They found that hydrophilic surfaces have a catalytic effect on GB degradation, whereas hydrophobic ones hinder the hydrolysis process by increasing the reaction barrier by ~10 kcal/mol (the reaction barrier in bulk water was ~50 kcal/mol). In case of a hydrophilic surface the reaction pathway is the same as in water solution, where the GB molecule is fully hydrated and proceeds via one-step reaction mechanism (Figure 3.11). Additionally, the reaction barrier was lower by ~15 kcal/mol and a hydrogen bond between GB and the adsorption sites on the surface limited GB mobility and prevented it from diffusing into the bulk aqueous phase.
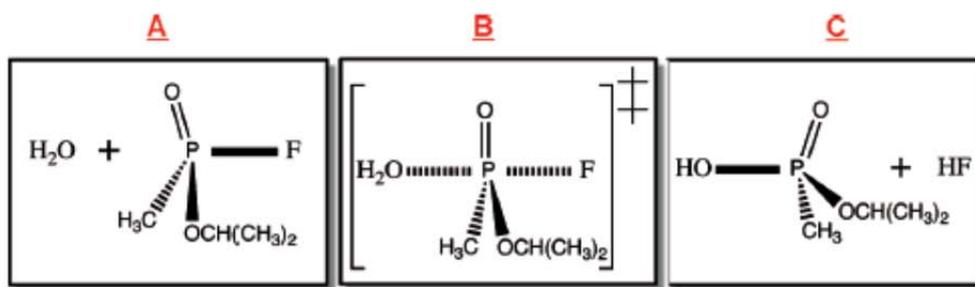
Figure 3.11 Scheme of sarin degradation near hydrophilic surface. Reaction proceeds via S_n2 mechanism, where an intermediate is formed via nucleophilic attack from water molecule [34].

When a hydrophobic surface was employed, a two-step reaction mechanism was observed, where fluorine-phosphorus bond breakage was followed by oxygen-phosphorus bond formation, with oxygen provided by a neighboring water molecule (Figure 3.12).
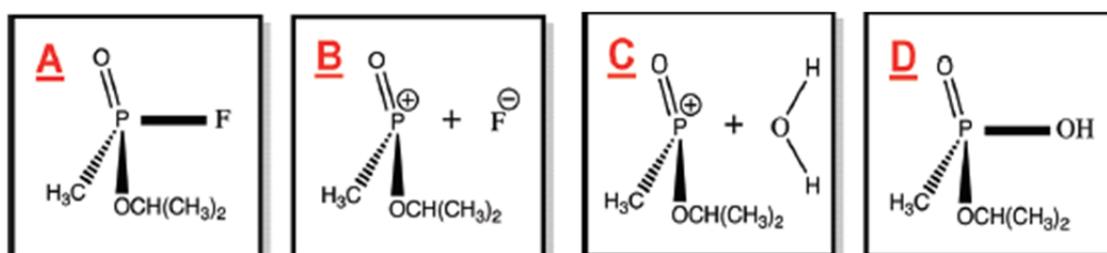

Figure 3.12 Scheme of sarin degradation near hydrophobic surface. Reaction proceeds via S_n1 mechanism where two intermediates (B and C panels) are formed [34].

3.3.6 Omniphobic surfaces

Table 3.1 shows contact angles of water droplet on materials with different surface energy. As one can see high contact angles can be achieved for liquids with high surface tension, such as water, resting on a solid with low surface energy. On the other hand, organic liquids, including CWA have much lower values of surface tension (Table 3.2). Therefore it is possible to achieve high contact angle only in case of the solid with surface energy comparable to surface tension of a liquid.

Surfaces which cannot be wetted by both water and organic liquids are called **omniphobic** since they are both oleophobic (oil-repelling) and hydrophobic. Omniphobic surfaces have attracted much attention, since they could be used to prevent surface contamination. In a solicitation number W911QY12S0411, issued on 11th April 2012 the US Army calls for an omniphobic coating which could be used in the military clothing to "*help to protect the skin from contact with solid and liquid toxic industrial chemicals, petroleum, oil, and lubricants, chemical warfare agents, and bacteria and viruses, thus effectively providing enhanced chemical/biological (CB)*

protection" [35]. In addition to omniphobicity the coating should also possess, among other properties, appropriate mechanical strength and flexibility.

Table 3.1   Contact angles of water at 20ºC with solids of different surface energies [36]

Material	Surface energy [mJ/m^2]	Contact angle [°]
Clean glass	73	0
Platinum	62	40
Anodized aluminium	50	60
Polymethyl-methacrylate (PMMA)	41	74
Nylon	38	79
Polyethylene	33	96
Polypropylene	26	108
Paraffin	19	110
Teflon	18	112

Table 3.2   Surface tension values for water and different CWA [4].

liquid	Surface tension 10^{-3}N/m (at 25ºC)
Water	72.8
HD	42.5
GA	32.5
GB	25.9
GD	24.5
GF	32.3
VX	31.3

Polymers are among solids with lowest surface energy (solid surface tension). Wettability of polymers was studied by Zisman [24], who discovered that for low energy solids relation between $cos\theta$ vs. γ_{lv} is linear (unless hydrogen bonds are forming between liquid and solid):

$$cos\theta = a - b\gamma_{lv} = 1 - \beta(\gamma_{lv} - \gamma_c) \tag{3.9}$$

γ_c is called the critical surface tension of a solid and is characteristic property of any given solid. Liquids with $\gamma_{lg} > \gamma_c$ will wet the surface of a solid, and for polymers it is found that $\gamma_c \approx \gamma_{sv}$. An example of the so-called "Zisman plot" is shown in Figure 3.13.
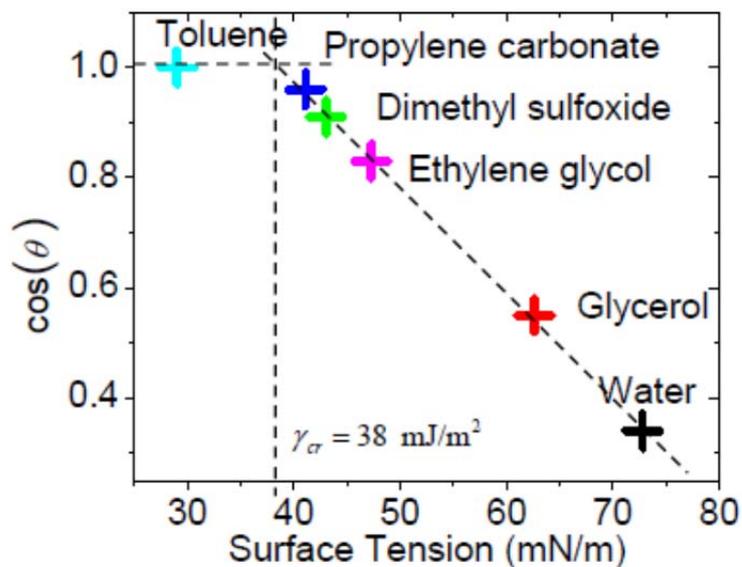
Zisman plot for PMMA using various testing liquids

Figure 3.13 Zisman plot for PMMA (γ_c=38mN/m) for various liquids[37]

According to Zisman the wetting properties of polymer surfaces stem from the surface composition, which can be represented by the horizontally oriented polymer molecule. Therefore the surface tension depends on the constituent groups. For hydrocarbons, surfaces consisting of close-packed, oriented methyl groups have lowest values of γ_c, whereas for halogenated polymers it was found that surface comprising of close-packed CF_3- groups was much less wettable than CF_2- groups. Values of surface tension for halogenated polymers are presented in Table 3.3. Interestingly, a condensed monolayer of perfluorolauric acid $F_3C(CF_2)_{10}COOH$ was "*the most unwettable surface ever reported; on it every liquid we studied was unable to spread*" [24]. Such observation is particularly interesting from CWA's protection point of view and one can expect the omniphobic properties being based on CF_3-containing polymeric coating applied to the surface.

Table 3.3   Critical surface tensions of halogenated polyethylenes [24].

Polymer	Structural Formula	Critical surface tension, Dynes/cm
Poly(vinylidene chloride)	H Cl H Cl H Cl —C—C—C—C—C—C— H Cl H Cl H Cl	40
Poly(vinyl chloride)	H Cl H Cl H Cl —C—C—C—C—C—C— H H H H H H	39
Polyethylene	H H H H H H —C—C—C—C—C—C— H H H H H H	31
Poly(vinyl fluoride)	H F H F H F —C—C—C—C—C—C— H H H H H H	28
Poly(vinylidene fluoride)	H F H F H F —C—C—C—C—C—C— H F H F H F	25
Polytrifluoroethylene	F F F F F F —C—C—C—C—C—C— H F H F H F	22
Polytetrafluoroethylene (Teflon)	F F F F F F —C—C—C—C—C—C— F F F F F F	18

Somehow similar approach was recently demonstrated by Wong et al [1], who used a nano- and microstructured surfaces to immobilize the lubricating fluid, which would yield an omniphobic surface resistant to liquid pressure changes (Figure 3.14). As a result the surface exhibits extraordinarily low surface energy which makes it repel practically any liquid. The so-called SLIPS (**Slippery Liquid-Infused Porous Surfaces**) were fabricated from different substrates including Teflon membrane showing random or oriented roughness and commercially available perfluorinated fluids (Figure 3.15). The authors in a series of experiments showed that this surface treatment allows for maintaining low contact angle for variety of liquids regardless of their surface tension and can be applied to several low-surface-energy materials. It also shows self-healing properties and can be made transparent. Apart from outstanding abilities of restoring

its liquid-repelling properties in case of damage by abrasion or impact, SLIPS showed excellent omniphobicity and hydrophobicity also upon exposure to high pressure, which during the laboratory tests was equivalent to hydrostatic pressure at a depth of ca. 7 km (Figure 3.15).
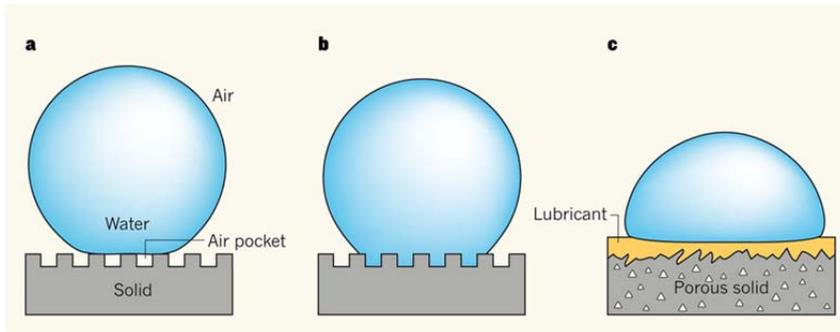

Figure 3.14 Comparison of Cassie-Baxter (a), Wenzel (b) and SLIPS (c) models of wetting [38]
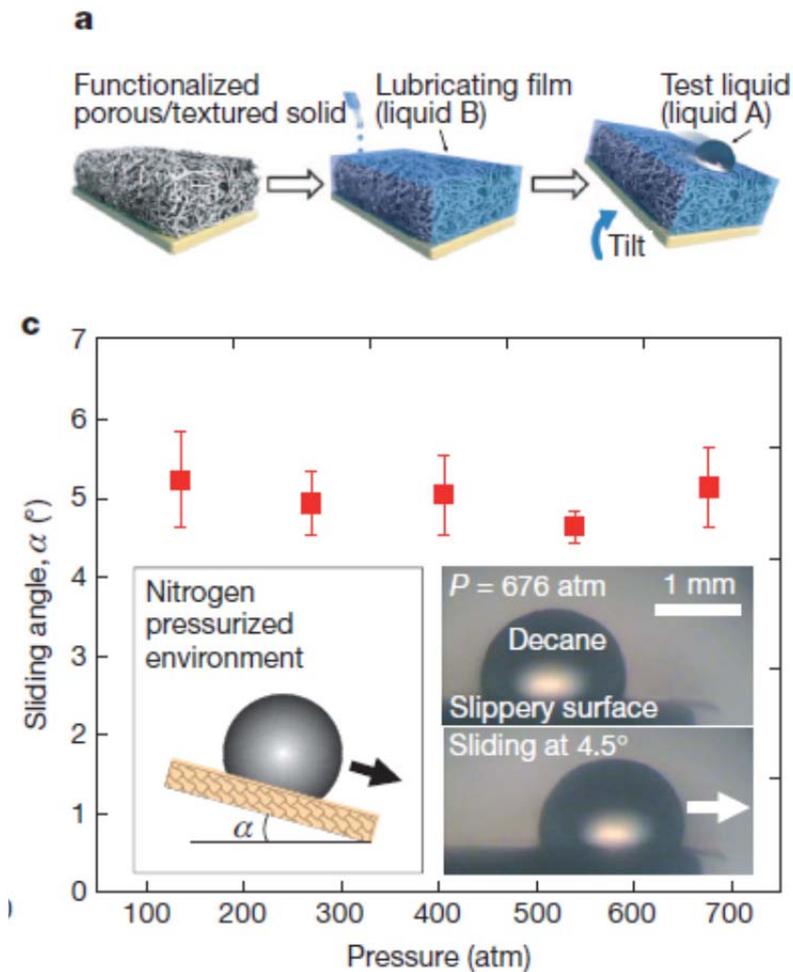
Figure 3.15 (above) Scheme of SLIPS fabrication, (below) Plot showing the high pressure stability of SLIPS, as evident from the low sliding angle of a decane droplet in a pressure chamber filled with nitrogen [1].

In a very recently published article (June 2012) the SLIPS technology was also shown to be useful in developing the coatings which can be applied to metal surfaces in order to suppress ice and frost accretion (icephobic coatings) [39]. Modified surfaces held their superhydrophobic properties even in high humidity conditions. Moreover, the surfaces exhibit much lower ice adhesion, so that in ultra-frigid conditions, any ice forming easily slides away with help of gravity or air stream. Potential applications include, among others, refrigeration, aviation, wires and wind turbines.
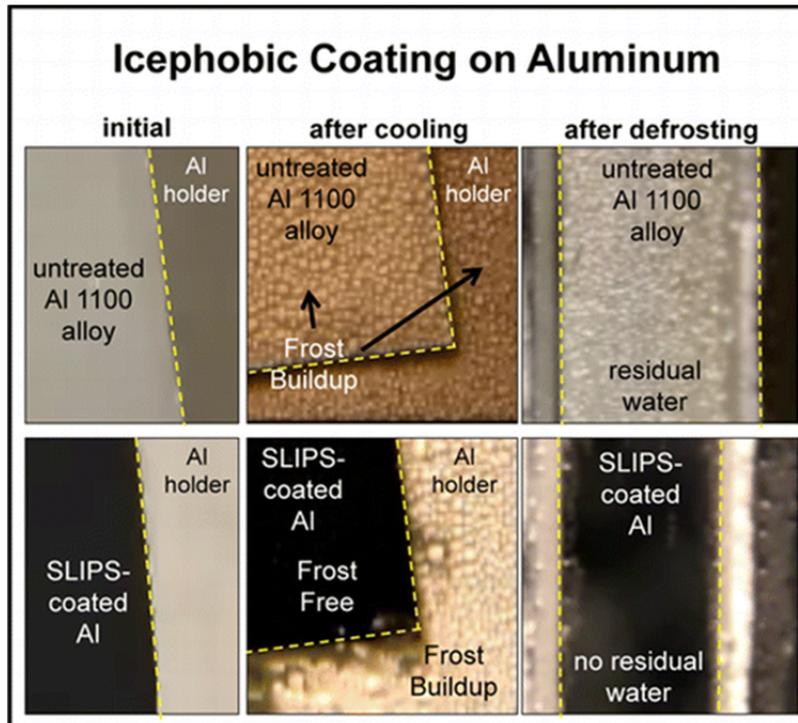
Figure 3.16 An example of SLIPS technology for anti-frosting applications on industrially relevant metals [39].

3.3.7   Evaporation rate vs. droplet curvature

The surface tension causes a droplet to shrink, and at the same time the internal pressure is increasing. As a result the pressure inside the droplet is higher than outside. This pressure difference is given by Laplace equation [23]:

$$p_{in} = p_{out} + \frac{2\gamma}{r} \qquad (3.10)$$

As a consequence the vapor pressure over curved surface will be different than over flat one. Vapor pressure of a liquid when it is dispersed as droplets of radius *r* is given by Kelvin equation [23]:

$$p = p' e^{2\gamma V_m / rRT} \qquad (3.11)$$

where p' is vapor pressure of a liquid, V_m is molar volume; R is the universal gas constant and T is temperature. The pressure above the surface of a droplet with smaller radius is higher than above one with greater radius; consequently the evaporation rate for small droplets will be higher than for the big ones.

3.3.8 Droplet formation and spreading

Liquid CWA are often employed as aerosols, i.e. a suspension of droplets in a carrier gas. Formation of the CWA droplets, their spreading and fate (absorption, evaporation) has been a subject of both experimental and theoretical studies, and many aspects of the liquid-solid interactions can be modeled, analyzed and described in terms of fluid mechanics. In general, when those droplets collide with a surface of a rigid solid they may spread, splash or bounce back, depending on the droplet kinetic energy upon impact and the surface tension of a liquid [40]. When a droplet spreads, a thin film of liquid is formed on the surface, whereas splashing results in formation of a crown and secondary droplets (Figure 3.17). The maximum spreading diameter depends on the droplet characteristics (volume, impact momentum on the surface, viscosity and density of the liquid) and the surface properties (roughness, hardness and hydrophobicity) [41, 42].

| Deposition (drop oscillates a little) | Prompt splash | Corona splash | Partial rebounding | Complete rebounding |
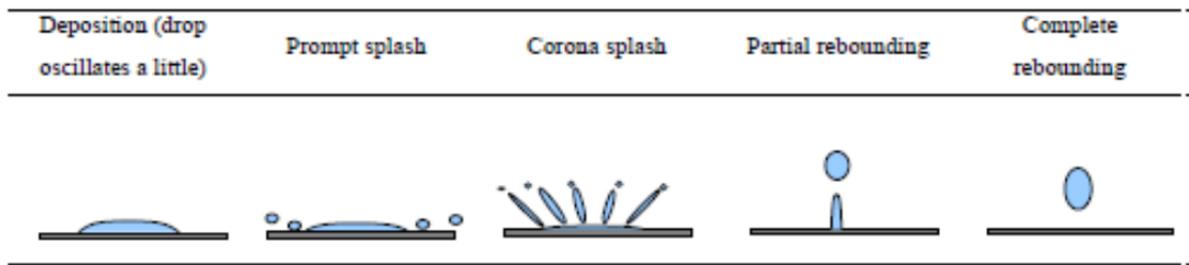
Figure 3.17 Observed behaviors of a droplet impacting on a solid surface [36].

A droplet-surface interaction is governed by the following dimensionless variables [40]:
Weber number, *We,* describes the importance of inertial effects in the flow to surface tension:

$$We = r_d \frac{\rho v}{\gamma^*} \tag{3.12}$$

where r_d is the droplet diameter, ρ is the liquid density, v – droplet velocity at impact, $\gamma*$ is the equilibrium surface tension of the interface between liquid and solid.
Reynolds number (*Re*) characterizes the importance of inertial effects in the flow to viscous ones. In brief, inertia is the resistance of an object in motion against a change in its velocity, whereas viscosity is the internal liquid resistance to flow. *Re* for a falling droplet is given by:

$$Re = \frac{r_d \rho v}{\mu} \tag{3.13}$$

where μ is dynamic viscosity of a liquid. Reynolds number is used to determine whether the flow is laminar or turbulent. For a laminar flow (low *Re*) of a fluid along the pipe all particles of fluid

are moving in straight lines parallel to the pipe walls, whereas in turbulent flow (high *Re*) their movement is in different directions.

Reynolds and Weber number are useful in predicting the behavior and the consequences of a droplet collision with a solid, such as the splash occurrence and the maximum spread. The transition from spreading to splashing is described by the following correlation:

$$ReWe = K \tag{3.14}$$

where *K* is a function of surface roughness of the substrate [40].

Sikalo et al. studied the droplet impinging on the horizontal surfaces for liquids with different viscosity and surface tension [42, 43]. Their results show that the maximum spread increases with increasing Reynolds number and Weber number [43]. Similar results were collected by Comeau et al., who studied the water droplet behavior as a function of *We* by increasing the initial height at which the droplet was released onto the surface (Figure 3.18) [44].
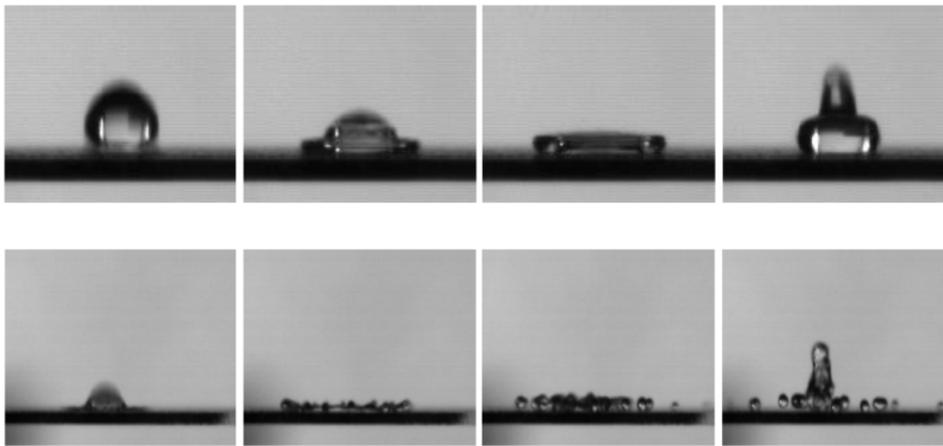
Figure 3.18 Water droplet impinging on a surface dropped from a height of 33 mm (top) and 145 mm (bottom) on a hydrophobic surface. In the first case droplet spreads before retracting and forms a Worthington jet; in the second it splashes and forms several secondary droplets before rebounding [44].

It was observed that splashing occurs at a certain critical value of Weber number [43]. It was found that the critical *We* value decreases with decreasing surface tension and increasing surface roughness, the last one affecting the maximum and final spreading diameter of a droplet. However, the final prediction of the droplet behavior is strongly influenced by the substrate hydrophobic or hydrophilic properties. Generally, an impinging droplet will spread immediately on the hydrophilic surface, but on the hydrophobic one it can reach the maximum diameter and then retract (Figure 3.19). Finally, for a certain values of *We* it is possible that the droplet colliding on a hydrophobic surface will bounce back without wetting the surface.

(a) $t = 0\text{ms}$ (b) $t = 2\text{ms}$ (c) $t = 4\text{ms}$

(d) $t = 7\text{ms}$ (e) $t = 11\text{ms}$ (f) $t = 14\text{ms}$
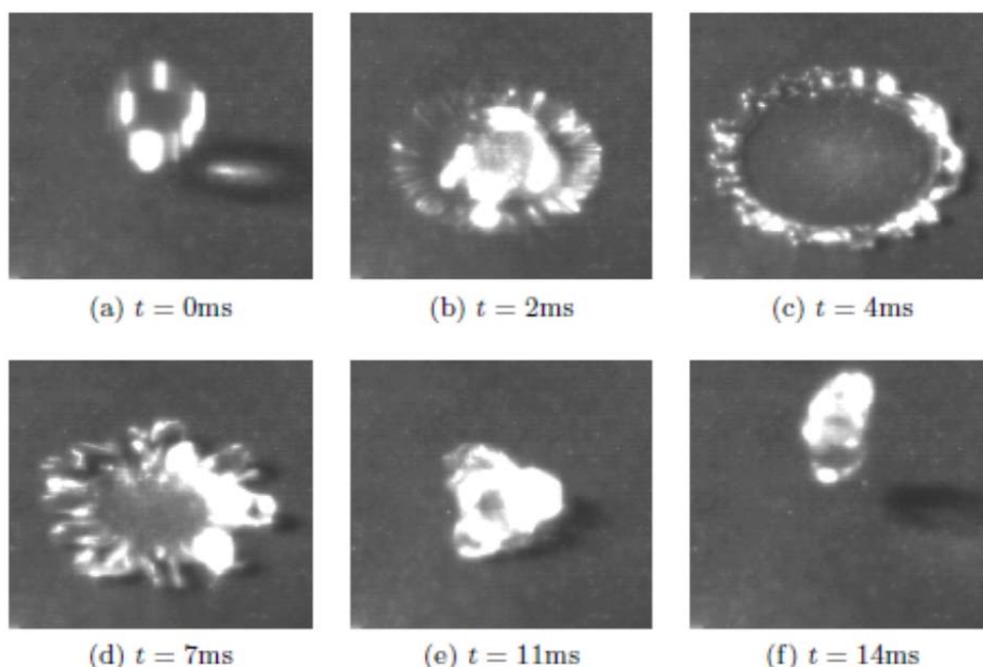
Figure 3.19 Impact of a water drop released from the threshold height of 100 mm viewed from the above [45].

3.3.9 Permeability and absorption

In case of a solid which can be penetrated by the liquid the physical processes of most importance include permeation, absorption and chemical reactions with the surface. Permeation is a process upon which a gas, liquid or solid penetrates through a solid, and consists of three stages: adsorption of diffusing substance, diffusion through the solid and desorption. The diffusion process is governed by the Fick's law:

$$J = -D\frac{\partial c}{\partial x}$$

(3.15)

where J [mol/m^2·s] is flux (amount of substance that will flow through an area during certain period of time, c – concentration of diffusing substance, x – the position of at a given time, D – diffusion coefficient, depending on the diffusing substance and the penetrated medium, temperature and in some cases concentration. The driving process for the diffusion is the chemical gradient arising from difference in concentration on the phase boundary.

Depending on the ability of the material to transmit fluids it can be described as permeable or non-permeable. Permeable materials often contain a network of pores or voids connected with each other, which can be entered by the liquid. Another important phenomenon which may occur during interaction between liquid and porous solid is absorption - the process upon which the liquid (or other phase) is taken up by the bulk of another. The liquid may then leak through the

material, or diffuse back out to evaporate (desorption), which in case of CWA will result in further contamination.

For an impermeable solid the droplet spreading and the final wetted area is governed mainly by the surface tensions of the liquid and the solid, which determine the contact angle between them and the resting droplet geometry and, in case of impinging droplet, its initial kinetic energy. However, in the case of a permeable substrate a droplet of liquid spreads in the lateral direction and at the same time penetrates the porous medium. Pores are usually sufficiently small in diameter to be considered as an array of capillary tubes, and the interactions between the liquid and the walls of the capillaries will be determined by the phenomena such as wetting [46, 47]. In particular, the higher the wettability, the more liquid spreads over the surface, and the higher liquid infiltrates the substrate, as the capillary pressure pulls it inside the pores. On the other hand, surface tension counteracts the spreading, so that the final spread diameter and the penetration depth is the result of these forces. Apart from capillary transport, other mechanisms controlling the temporal and spatial distribution of the droplet include phase change (evaporation or solidification), physical bonding (adsorption), and/or chemical reaction [48]. The laminar flow of a liquid through a porous medium is described by empirical Darcy's Law, where the rate at which a liquid flows through a porous medium is directly proportional to pressure difference between two places in the medium and inversely proportional to the distance between them:

$$Q = -\frac{kA}{\mu}\frac{(p_1-p_2)}{l} \tag{3.16}$$

where (p_1-p_2) is the pressure difference, l is the distance, k is permeability [m^2], A is the cross-sectional area, μ is the liquid viscosity and Q is the total discharge of a liquid. Permeability reflects the resistance the medium shows towards liquid permeation and is often expressed in darcy units.

3.3.10 Droplets on porous surfaces

The following considerations are carried for liquids which fully or partially wet the surface of solids. For a droplet infiltrating a porous medium two stages can be distinguished. The primary infiltration occurs while there is a volume of free liquid present on the surface, and secondary when there is no liquid left on the surface. Apart from a contact angle between solid and liquid, a dynamic contact angle (defined as a tangent angle on the sessile droplet shape) can be distinguished, as the droplet decreases in volume due to infiltration (
Figure 3.20).
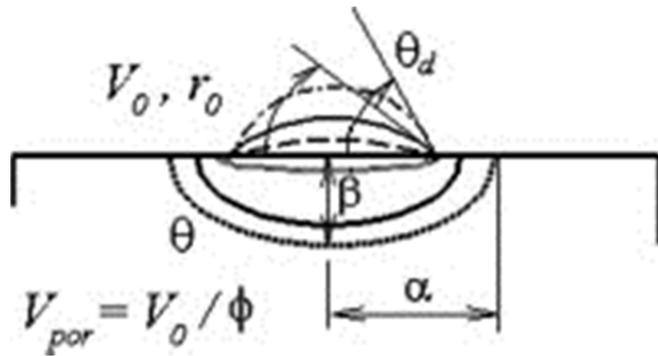
Figure 3.20 Spread of the sessile droplet of initial volume V_0 and base radius r_0 into homogenous porous medium for constant r_0 value. The imprint volume $V_{por}=V_0/\phi$, θ is the contact angle, θ_d - dynamic contact angle; α, β – imprint haf-axes [46].

Spreading of the sessile droplets into porous media was studied by Navaz and Markicevic, who successfully simulated the primary and secondary infiltration of droplet in porous media using both numerical methods and experiments [46, 48-50]. They observed that secondary infiltration was affecting to a large extend the imprint of the droplet (i.e. wetted volume in a porous medium), and the liquid kept spreading inside the solid after the free volume on the surface was gone. As some parts of a liquid detached from the droplet front, the process continued until the isolated parts of the liquid phase stabilized and the capillary pressure inside the pores did not cause further infiltration. Interestingly, the capillary pressure showed dependency on medium homogeneity but seem independent on the droplet size. The authors determined experimentally the capillary pressure values of various liquids, including VX and HD, in consolidated (sand, glass beads) and unconsolidated (ceramic tiles) media of different porosity [50]. The data were then used in the numerical simulations. The imprint shape and the penetration depth obtained from the simulation showed quantitative and qualitative agreement with the experimental results, thus proving the usefulness of the method in predicting the liquid infiltration in porous medium.

When a droplet has an initial kinetic energy due to e.g. free fall from certain height, the spreading on and inside the substrate will be affected not only by the capillary forces but also by the droplet momentum and the pressure applied to the surface by the falling droplet. Figure 3.21 presents schematically the comparison between geometry of a droplet impinging on smooth, solid, impermeable (a) and permeable (b) substrates [51].
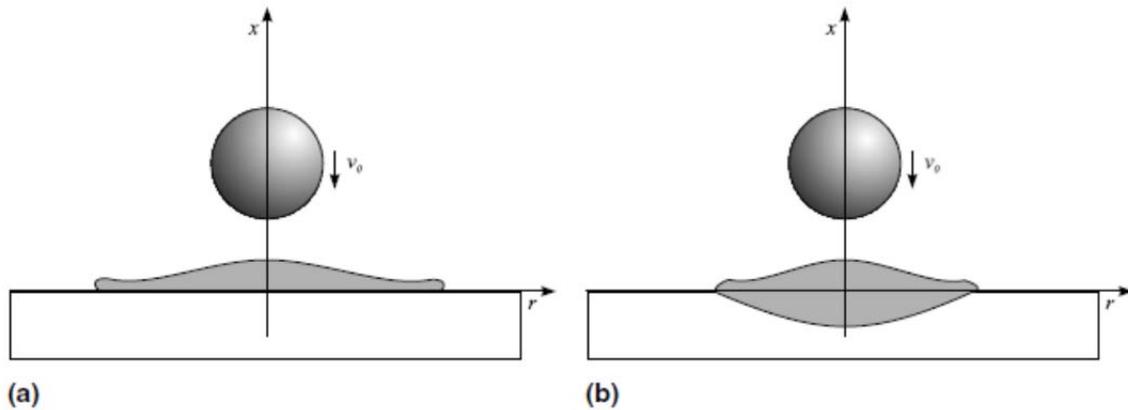
Figure 3.21 Schematic representation of the droplet impinging on a flat, non-permeable (a) and permeable (b) surface [51].

The mechanism of liquid droplet spreading in case of porous (permeable) and impermeable surfaces was investigated by Reis et al. by means of numerical simulations and NMR imaging [47, 51]. Possible spreading scenarios were analyzed by varying i.a. values of Reynolds, Weber and Darcy numbers[2], contact angle and the substrate porosity. Reys et al. noticed a substantial reduction in droplet lateral spreading as compared to the one for impermeable substrates and assigned it to the smaller pressure at the impact region due to liquid movement across the liquid-solid interface [51]. Subsequently the lateral spreading becomes slower with time, mostly due to the viscosity of the liquid and the reduction of velocity with the increasing droplet radius, so that the condition of mass and momentum conservation is fulfilled. The velocity of the movement towards the bulk of the substrate will be related to the initial axial momentum of the droplet, pressure imposed by the liquid onto the surface and the capillary forces dragging the liquid inside the pores. An example of the time evolution of the impinging droplet shape and spatial distribution inside porous media of different porosity (given as a ratio of pores volume to the total volume of the medium) is shown in Figure 3.22 [47].

---

[2] Darcy number is a dimensionless parameter introduced to reflect the permeability of porous medium by a droplet of liquid and defined as $D_a = \frac{k}{r_0^2}$, where k is permeability and r_0 the initial droplet radius [47].
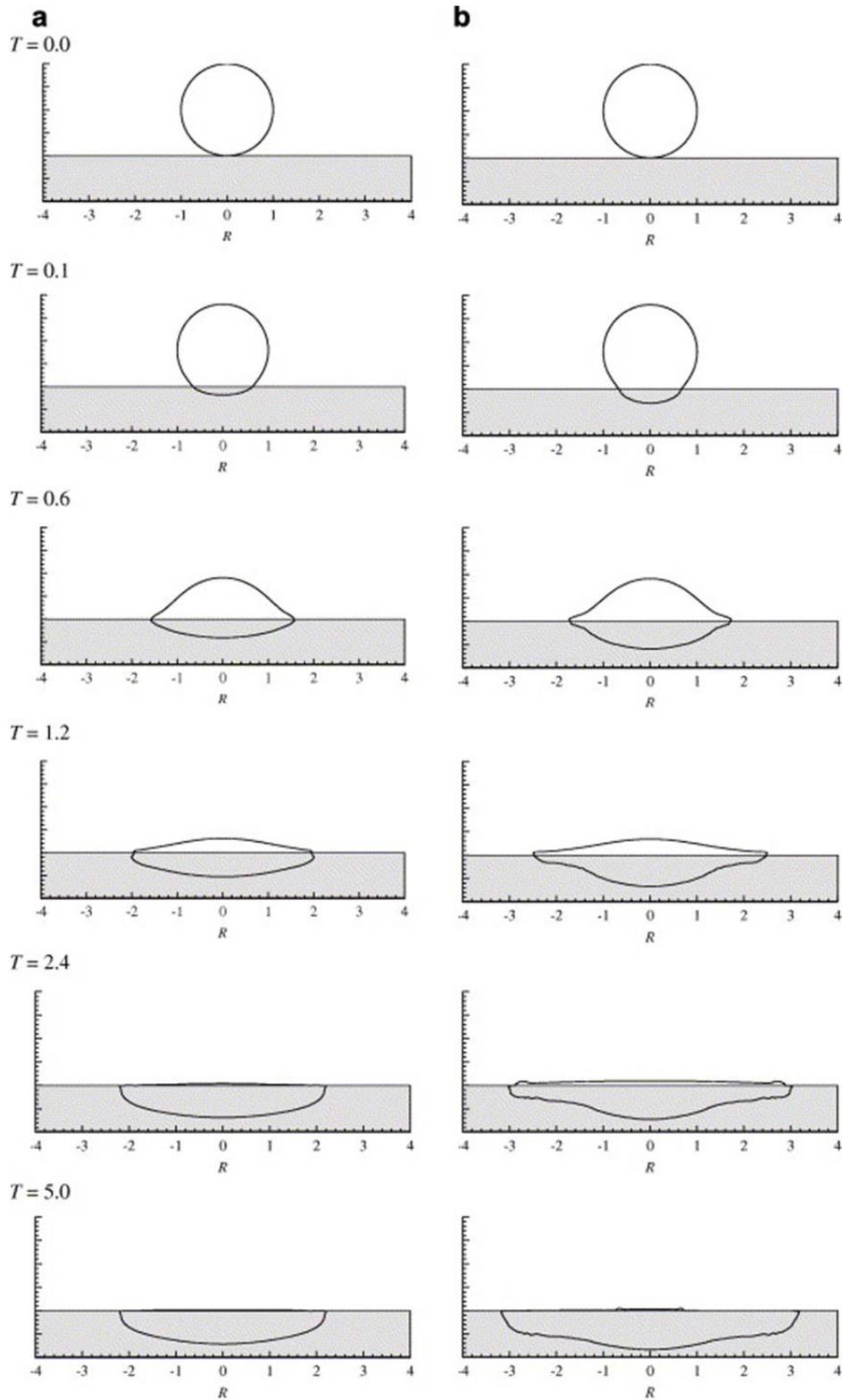
*Figure 3.22 The imprint of a falling droplet in substrates with 0.55 (a) and 0.25 (b) porosity. The less porous medium has smaller available volume for the liquid and it tends to penetrate larger volume of a substrate [47].*

It is important to note that in certain scenarios the rate of permeation will be comparable to the rate of evaporation of the liquid. Moreover the evaporation will be now affected not only by the

droplet curvature, but also the shape and diameter of the meniscus of the liquid inside the pores of a solid. For CWA this will have a significant impact on their persistency in and over the porous medium.

3.3.11 Evaporation from permeable and non-permeable solids

The evaporation of CWA is often studied using the wind tunnels of different geometry in order to collect the data useful for modeling and predicting the consequences of a real scale CWA contamination [52, 53]. Many models presented in general literature concern the scenario where evaporation source is represented by a pool of liquid and free-surface evaporation is investigated. At FFI different models evaporation with regards to CWA and toxic industrial chemicals (TIC) were developed and studied experimentally and by means of numerical simulations [54-57]. It should be noted that good quality experimental data necessary to develop and evaluate such models for CWA are restricted and therefore cannot be accessed from public sources.

The droplets evaporation is often studied for the case of spreading of liquid fertilizers over agricultural area or printing technology (jet-ink printers). Apart from physical and chemical properties of the liquid and the ambient conditions (wind speed, temperature etc.) the evaporation rate will also depend on the geometry of the droplet, as it is shown by Kelvin equation. For a droplet two possible mechanisms are distinguished (Figure 3.23):

- droplet maintains constant contact angle – the evaporation rate is changing throughout the process, as the droplet surface area is decreasing
- droplet maintains constant contact area – the surface area changes very slightly, therefore the evaporation rate remains constant
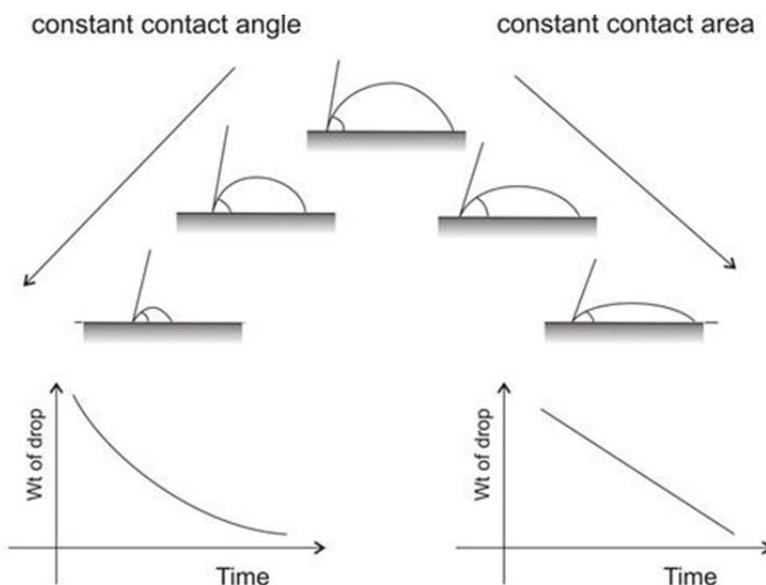

Figure 3.23 Schematic representation of HD evaporation process from inert, non-porous surface [52].

During the evaporation from the porous surface two distinct stages are observed. Either the surface is saturated with the liquid (pores are full), or there is still a free volume of the liquid on the surface. In such a case the evaporation proceeds via vapor transport by the surrounding air stream. Under steady atmospheric conditions the evaporation rate is then constant (constant-rate period). In the second stage the liquid disappears from the surface and the pores, so the evaporation front is moving into the substrate. The evaporation rate will then depend more on the molecular transport of liquid through the pore network (falling-rate period) [53]. For unconsolidated substrates – such as sand – where the pore network typically consists of large, interconnected voids a fast permeation and evaporation can be expected, since the interconnecting capillaries do not inhibit vapor or liquid flow. Conversely, sluggish permeation and evaporation can be observed in case of consolidated solids with fine pores, like concrete or asphalt. The evaporation of CWA from soil, sand, concrete and asphalt was modeled by Westin et al. [58], who obtained fairly good agreement between model and experimental results, especially for longer periods of time.

4   Interaction with materials

Numerous studies were done addressing the scenarios of CWA contamination on various indoor and outdoor materials, such as concrete, metals, ceramic tiles, plastics, rubbers, wood etc. Typically the aim of those studies was to investigate the persistency of CWA and efficacy of chosen methods of decontamination.

US Environmental Protection Agency (EPA) has published several reports on CWA interaction, with materials, e.g. in case of indoor contamination, where coupons of commercially available items were spiked with persistent CWA and analyzed in terms of CWA uptake and decontamination efficiency [59]. In general CWAs are most persistent on the porous materials, the inorganic ones being easier to decontaminate. Figure 4.1 presents the general persistency of liquid CWA on the surfaces of different materials used in indoor and outdoor civilian environment, depending on their porosity and chemical composition.
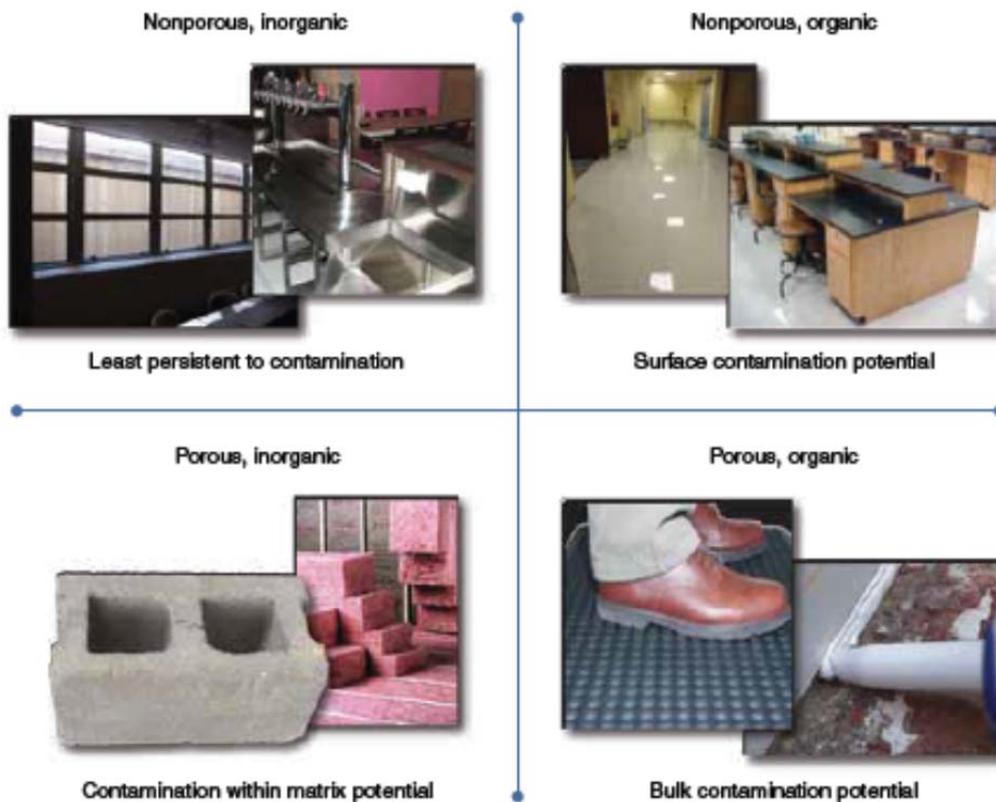
Figure 4.1   General sorption and decontamination characteristics of commonly used materials exposed to CWA [60].

Data on absorption characteristics of different classes of materials can also be found in NATO documents (Table 4.1) [61]. This information is relevant from practical point of view; however it does not provide the mechanisms of CWA uptake and physical and chemical reactions with the materials. In particular, possible predictions of the penetration depth of the agent into the material, its movement across the substrate and chemical reactions with the surrounding matrix can be of interest for the proper assessment of the consequences of CWA contamination and decontamination procedures. The following sections contain the literature data on the CWA penetration, spreading and degradation mechanisms in selected materials common in urban environment.

Table 4.1   General absorption characteristics of chosen materials.

Material	Sorption/permeation properties	Comments
Bare metals, glass, glazed ceramics	Impermeable	Easy to decontaminate. Corrosion products may appear on bare metal.
Finishes	Absorption (alkyd and acrylic paints)	Possible vapor desorption for up to several weeks. Catalytically hardened (epoxy paints, polyurethane) are less permeable.
Fabrics (canvas, cotton, wool, leather)	Rapid absorption	Chemical corrosion. Coatings or laminats (butyl ruber, Teflon) reduce permeability. Impossible to decontaminate.
Wood	Absorbent	Chemical finishing decrease absorption. Impossible to decontaminate.
Rubbers	Various. Fluorinated (Viton) and butyl most resistant, silicon most permeable	
Plastics	Various	Depends on the manufacturer, physical properties, and chemical composition.

4.1   Concrete

Concrete is one of the most popular materials in building and road construction industry. It consists of cement, sand, water and aggregates (gravel, crushed stones). Concrete is a ceramic material with a high surface energy due to covalent and ionic bonds, but it also shows certain porosity allowing for penetration of CWA into its structure. Cement, which accounts for approximately 10 to 15% of concrete, is a mixture of calcium compounds and oxides of silicon, aluminum and iron. Depending on the composition there are different types of cement available. Table 4.2 presents chemical composition of one of the most often used types of cement, Portland cement [62] .

Table 4.2   Example of a phase composition of Portland cement [62].

Cement compound	Weight percentage	Chemical formula
Tricalcium silicate	50%	Ca_3SiO_5 or $3CaO \cdot SiO_2$
Dicalcium silicate	25%	Ca_2SiO_4 or $2CaO \cdot SiO_2$
Tricalcium aluminate	10%	$Ca_3Al_2O_6$ or $3CaO \cdot Al_2O_3$
Tetracalcium aluminoferrite	10%	$Ca_4Al_2Fe_2O_{10}$ or $4CaO \cdot Al_2O_3 \cdot Fe_2O_3$
gypsum	5%	$CaO \cdot 2H_2O$

Once cement is mixed with other concrete ingredients, its constituents start reacting with water in a process called hydration. Different compounds react with different rate, which affects the mechanical strength of the concrete, and some of the reactions are so slow that they proceed many years after the concrete was made. Hydration reactions of tricalcium silicate and dicalcium silicate, which are the main phases in cement, are given in reactions 1 and 2.

$$2Ca_3SiO_5 + 7H_2O \rightarrow 3CaO \cdot 2SiO_2 \cdot 4H_2O + 3Ca(OH)_2 \; ; \; \Delta E = +173 kJ \qquad (4.1)$$

$$2Ca_3SiO_4 + 5H_2O \rightarrow 3CaO \cdot 2SiO_2 \cdot 4H_2O + Ca(OH)_2 \; ; \; \Delta E = +58,6 kJ \qquad (4.2)$$
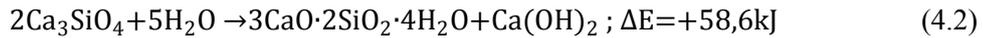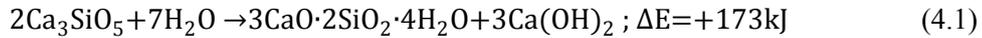
Tricalcium silicate reacts with water very rapidly and is accompanied by a substantial temperature increase, whereas dicalcium silicate hydration takes more time and less heat is evolved. Reactions of the other phases are more complex and proceed even slower.

As can be seen reactions (1-2) yield a substantial amount of calcium hydroxide, $Ca(OH)_2$, which forms crystals in the concrete microstructure. The $Ca(OH)_2$ content can be around 25% of the entire concrete volume. In presence of moisture $Ca(OH)_2$ will dissociate according to the reaction:

$$Ca(OH)_2 \overset{H_2O}{\longleftrightarrow} Ca^{2+} + 2OH^- \qquad (4.3)$$

The OH^- ions formed during hydration reactions are responsible for the alkalinity of concrete and they participate in the degradation processes of CWA observed on its surface, especially when humidity is present. However, as $Ca(OH)_2$ reacts with CO_2 from air (carbonatation; reaction 4), the pH of concrete decreases with time and its reactivity towards CWA will therefore decline.

$$Ca(OH)_2 + CO_2 \rightarrow CaCO_3 + H_2O \qquad (4.4)$$

4.1.1   Sulfur mustard on concrete

Mustard is reported to degrade upon contact with concrete surface, and the degradation products are analogical to those of hydrolysis reaction. Tang et al. [63] studied sorption, diffusion and degradation of distilled mustard on freshly prepared concrete samples. The samples used were pure cement type 425 purchased from Shuangshan Cement Company in Beijing mixed with water to form slabs.

The penetration time through a concrete slab was reported to decrease with increasing content of SiO_2 in the specimens. Simultaneously with diffusion through a slab degradation reactions occurred. The products of decomposition found by gas chromatography–mass spectrometry (GC-MS) are listed in Table 4.3. Apart from mustard (no.1) toxic 1,2-bis-(2-chloroethylthio)-ethane (Q or sesquimustard, no. 2), 1,4 - thioxane (no. 4) and bis-(2-chloroethyl)disulfide (no. 5) were found. The degradation of HD on concrete was associated with the presence of basic sites in concrete, i.e. $Ca(OH)_2$ phase formed during hydration.

The diffusion coefficient of HD in concrete D was found to be $2,2 \cdot 10^{-6}$ cm^2/s, and the degradation rate constant $k = 4,8 \cdot 10^{-5}$ min-1 and $t_{1/2} = 16 \cdot 10^4$ min (time when approximately 50% of HD is degraded) at room temperature.

Table 4.3   HD and products of its degradation on concrete identified by GC-MS [53].

no.	t_R (min)	Structural formula
1)	10.04	
2)	16.91	
3)	5.34	
4)	5.63	
5)	13.43	
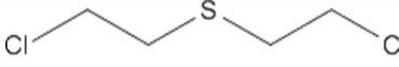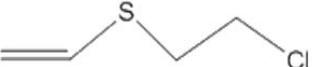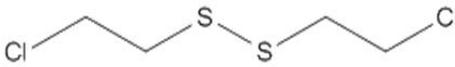
Brevett et al. studied HD degradation on ambient and moist concrete [64, 65] . In [64] 6 year old concrete monoliths made out of Portland cement, approx. 3 mm large grains of silicate filler and 0.32 water:concrete ratio were examined. 1H Nuclear Magnetic Resonance (1H NMR), 2D 1H-13C NMR, 13C solid state magic angle spinning NMR (SS-MAS NMR) and gas chromatography with mass selective detection (GC-MSD) were used for in situ and extraction analysis of mustard degradation products. When extraction and GC-MSD was used, the samples yielded a 90 – 100% HD recovery after 1 h and 40% after 48 hr. Depending on contact time and concrete:HD weight ratio different products were identified (Table 4.4).

Table 4.4 Products and the normalized response observed in the extracts of different concrete:HD ratio samples via GC/MSD [54].

Products and the normalized response observed via GC-MSD	24 h contact time			192 h contact time		
Concrete to HD ratio (weight)	55:1	77:1	198:1	47:1	86:1	234:1
2-Chloroethyl vinyl sulfide (CEVS)	2.3	3.3	4.0	1.3	3.7	4.9
2-Hydroxyethyl vinyl sulfide (HOEVS)		0.3	1.7	0.1	0.4	5.8
1,2-Bis(vinylthio) ethane (BVTE)			0.6		0.5	1.7
(2-Chloroethylthio)ethyl vinyl sulfide (CETEVS)				3.1	4.3	8.8

However, when SS-MAS NMR was used to examine *in situ* a ground sample of concrete (concrete:HD ratio 40:1), a combination of HD, H-2TG and (2-chloroethylthio)ethyl ether (T) was still present after 12 weeks. Further experiments proved that even after 12 weeks HD was still present in concrete, and the degradation products detected were described as potential vesicants and moderately toxic. According to reference [64] after 2 weeks HD binds to the concrete matrix and becomes non-extractable, causing considerable discrepancies between GC-MSD and NMR results.

The same group also examined concrete samples coming from an airport runway. The samples differed in age and pH [65]. When moist samples of concrete were used, the degradation of HD was much faster than on ambient ones (3.5% labile water content) [65]. Nevertheless, the degradation took place mostly on the relatively fresh samples of concrete. Samples age and properties are listed in Table 4.5.

Table 4.5 Physical properties of concrete samples used in degradation study [55].

	C04	C90	C03
Surface area [m^2/g] crushed/monolith	2.2/3.1	1.9/1.4	2.0/1.3
Crushed pH, 1/24 h	12.5/12.5	8.0/8.5	12.0/12.0
Monolith pH, 1/24 h	10.5/12.0	6.5/7.5	8.5/9.0
Age of sample when pH tested	6 months	Est. 10–20 years	1 year

At 22 °C on the ambient concrete the half-life[3] of HD molecules ranged between 3.5 and 54 weeks, whereas on moist concrete from 75 to 350 hr. From NMR results it was found that the HD degradation proceeds via intermediate sulfonium ions formation: CH-TG, H-TG, H-2TG

---

[3] The half-life corresponds to 50% of molecules undergoing degradation within given period of time.

(Figure 2.5) and 4-(2-hydroxyethyl)-1,4-oxathianium (HOEt-OT), which would decompose to the relatively non-toxic compounds: TDG, 1,4-oxathiane and 1,4-dithiane. On the other hand, the decomposition rate was slow and toxic sulfonium ions persisted for months to years on concrete at 22 °C and weeks to months on concrete at 35 °C. In case of fresh samples, vinyl moieties such as 2-hydroxyethyl vinyl sulfide (HOEVS) and 2-chloroethyl vinyl sulfide (CEVS) were also found as decomposition products (Table 4.6) [66]. An increase in temperature enhanced the degradation rate.

Table 4.6   Percent vinyl moieties for HD degradation on concrete [56].

Concrete sample	Temperature, ^{o}C	Ambient	Moist
C03	22	10	10
C90	22	0	0
C04a/b*	22	13/13	10/na
C04	35	18	11
C04	50	16	13

*C04b was tested 4 months after C04a

A long-term study (17 months) was performed by Mizrahi et al., who investigated HD degradation on aged ground concrete by ^{13}C SS-MAS [67]. They observed low degradation rate on dry concrete, where only 15% of HD degraded over 1 year to produce vinylic products via elimination route (Figure 4.). Degradation on wet concrete yielded multiple products: apart from HOEVS and CEVS, sulfonium ions, TDG and TDG oligomers were found, indicating that degradation occurred via both elimination and hydrolysis reactions. Analysis of kinetic data resulted in two half-lives of 72 and 162 days. The results confirmed those by Brevet et al. [65, 66], and the eventual differences in half-life times and products were accounted for the age of concrete used and different amount of water in concrete.
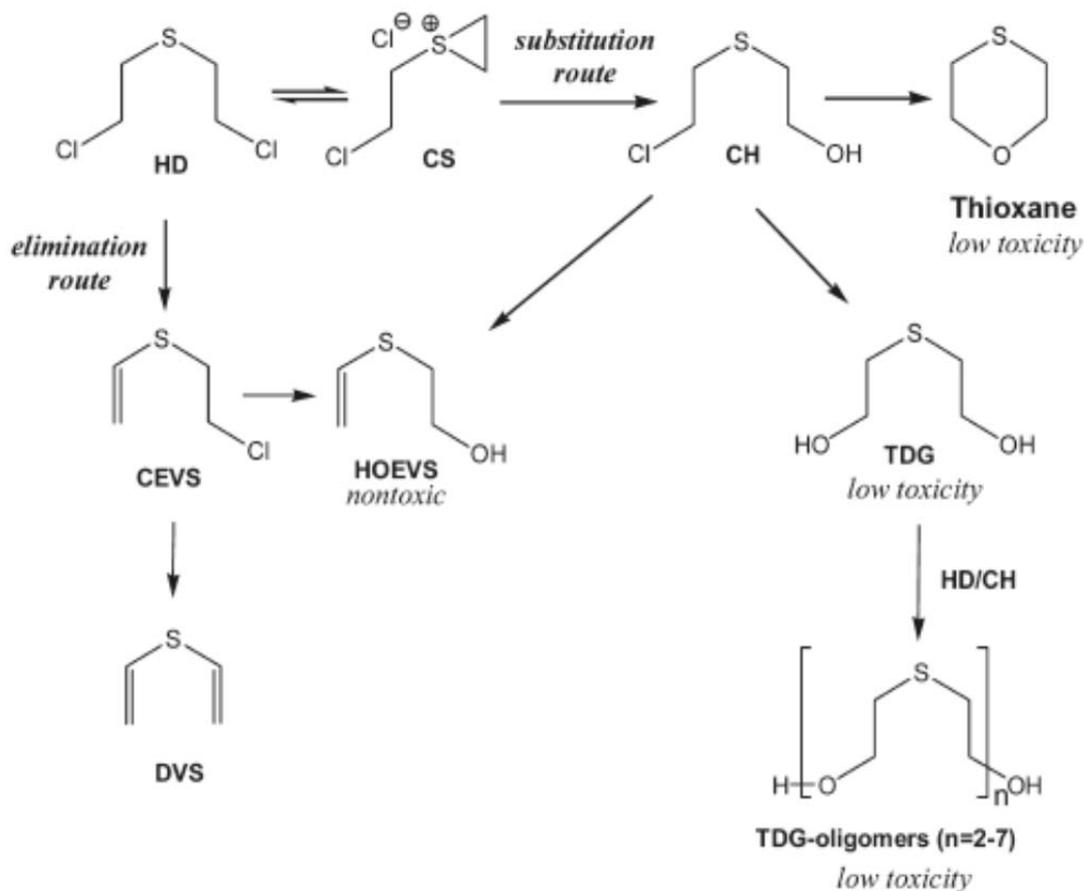
Figure 4.   Substitution and elimination routes of HD degradation [67].

4.1.2   VX on concrete

VX is found to be highly adsorptive to the surfaces and therefore difficult to remove. Since it is lethal in very small doses, the secondary contamination by desorption and evaporation or dermal contact with the affected surface is a serious threat. Therefore its fate on concrete surface, a common industrial and urban material, is of utter interest.

Groenewold et al. used Ion Trap Secondary Ion Mass Spectrometry (IT-SIMS) to study kinetics of VX degradation on concrete surface [68, 69]. A detailed description of IT-SIMS and the experimental setup can be found in reference [68]. Concrete was collected from the airport runway and spiked with diluted VX (powdered samples) or minute droplets of neat VX (chips) in order to achieve a monolayer coverage [68]. After one day VX could not be detected within the detection limit of IT-SIMS, which was 5 ng for chips and an equivalent of 0.0004 of monolayer for crushed concrete, respectively. The observed degradation products included EMPA, DESH, diisopropyl taurine (DIPT), bis(diisopropylaminoethane)disulfide [(DES)$_2$] and probably diisopropylvinylamine (DIVA). Interestingly, the latter could not be removed by extraction method and persisted over a week on concrete. Experiments was also carried out for powdered concrete samples of high pH from the Czech Republic (pH = 12 was measured for 35 g crushed sample immersed in 20 ml distilled water) [69]. In this case even shorter degradation time was observed (at 24 °C under experimental conditions VX would degrade to 1% of its initial

concentration within 15 h and to 1 ppm within 50 h). IT-SIMS results indicated that VX degradation proceeded via P-S and C-S bond cleavage, yielding 70% DESH and 30% diisopropylaziridinium (DIAZ), respectively. Toxic EA-2129 was not detected in any case. Rate constant at 24 ºC was k = 0.005 min^{-1}, and the activation energy was 52 kJ/mol, which is similar to that obtained for VX hydrolysis in alkaline solutions accompanied by DESH formation. However, it should be noted that a very small amounts of VX were used and the crushed samples were likely to be much more alkaline than the intact concrete.

Wagner et al. performed experiments on larger amounts of VX, aiming at more realistic conditions during the CWA attack [19, 70, 71]. Analyses of remaining VX and degradation products were done by ^{31}P NMR and ^{31}P MAS NMR. Much larger amounts of VX (15 µl on 737 mg chunk and 5 µl on 293 mg crushed concrete) were used. They found that VX is rapidly sorbed by concrete and degraded in a two-step reaction via selective hydrolysis and EMPA, DESH and (DES)$_2$ formation. Again, no toxic EA-2192 was detected. Initially about 12% of VX is decomposed via a fast reaction with a half-life of about 2.2 h, but the remaining VX phase is persistent with a half-life of 28 days to 3 months (Figure 4.2).
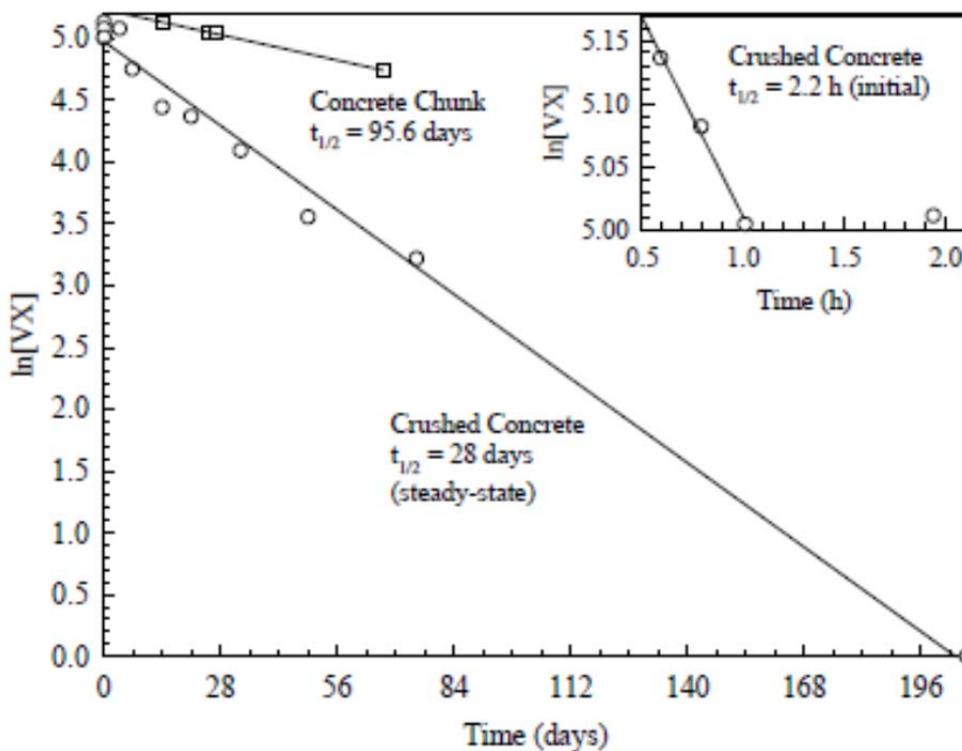
*Figure 4.2   Reaction profiles for VX sorbed in concrete. Inlet shows the initial fast reaction for VX on crushed concrete [70].*

The percentage of VX degraded during the fast reaction was almost identical with the amount accommodated on concrete as a monolayer, showing that concrete has limited reactive capacity. The authors speculated that a fast sorption mechanism of VX inside the concrete pores is caused

by reaction between excess VX, adventitious water and HCO_3^- ion from concrete carbonation, which would yield a protonated, solid $VX \cdot H_2CO_3$ specie (Figure 4.3).
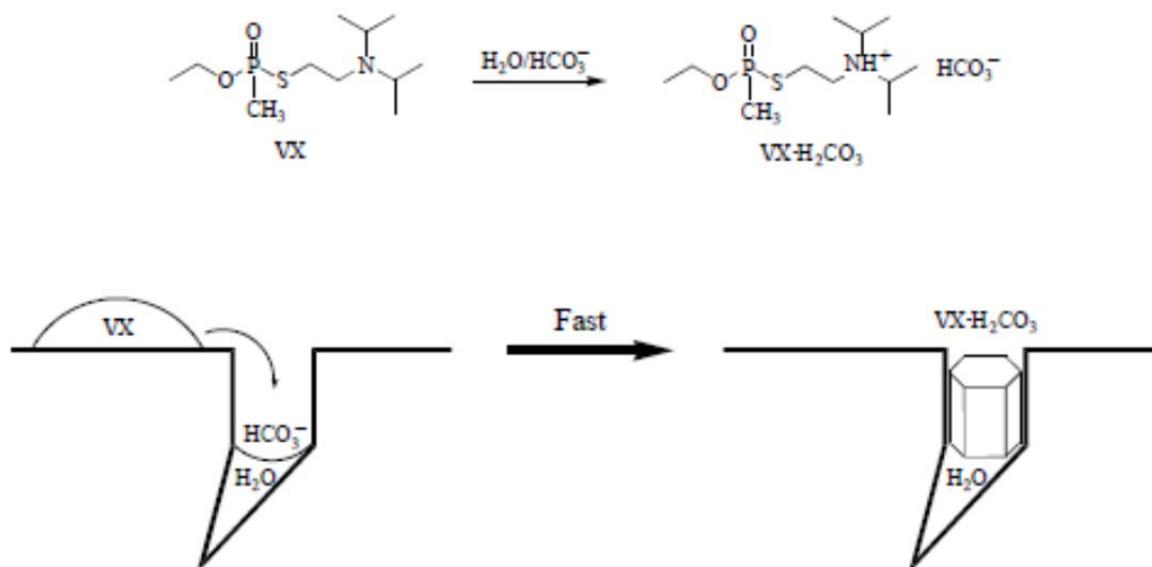
*Figure 4.3   Reaction scheme for VX sorption in concrete pores. VX reacts with adventitious water and HCO_3^- to form a solid protonated salt $VX \cdot H_2CO_3$ [70]*

An influence of droplet size on fresh and aged concrete was studied by the same group [19]. Neat droplets of VX were applied to coupons of "fresh" (2 months) and aged concrete (Figure 4.4). It was found that for 4 µl droplets VX was still detected after 4 days, whereas no VX was detected for smaller droplets after this period of time. Decomposition of VX to EMPA was observed. Additionally a 20 µl sample of diluted VX was also applied to achieve a uniform spreading of VX in the 14 month old concrete and compared with a droplet of neat VX of equimolar amount (4 µl). No significant changes between 14 months old concrete and "fresh" samples were found, but the aged concrete reacted much slower with VX. Possible explanation could be difference in pH of concrete (pH=10 for "fresh" and 14 months old, 9 for aged one). It was concluded that the dependence of VX decomposition on droplet size was caused by different spread diameter of the droplets. Although the global contamination level is the same for all cases and equals 17 mg/cm^2, the "local" contamination (spread diameter) will vary. On the basis of previous studies the authors related the local contamination values to the number of monolayers which would result from such loading. Since the number of monolayers was few orders of magnitude larger than the reactive capacity of concrete surface, droplets larger than 2 µl tend to persist on concrete, unless they were diluted to reach spreading comparable to smaller droplets.
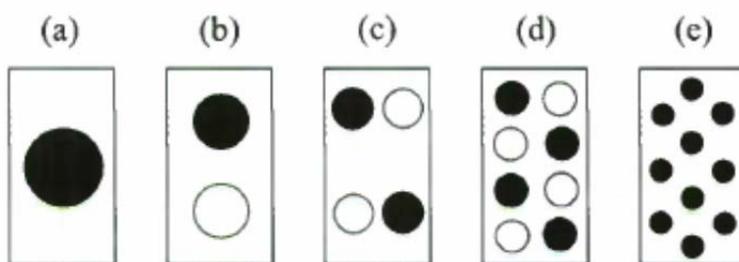
Figure 4.4   Patterns of neat VX drops applied to concrete coupons in Wagner et al. experiment [19]. (a)1 4 μl drop; 2 2.2 μl drops, (c) 4 1μl drops, (d) 8 0.5 μl drops and (e) 20 0.2 μl drops. Closed circles represent drops applied to the top face; open circles represent drops deposited on the bottom face. In (e), the same pattern was used on the bottom face, open circles have been omitted for clarity.

4.2   Polymeric materials and rubbers

Both absorption and permeation are observed for most rubbers and plastics. Polytetrafluoroethylene (PTFE), best known as Teflon is considered as impermeable. Most often the materials are tested against highly persistent agents such as HD and VX. Detailed procedures of testing the absorption together with the results for The detailed description of permeability and absorption tests of several rubbers, plastic and elastomers, together with the results for VX and HD can be found in reference [61].

In order to improve chemical resistance and impermeability of the polymers and rubbers different additives are used. Butyl rubber and silicone rubber are among the materials frequently used for military CBR respirators. These materials are thermosetting elastomers[4], which makes their processing more difficult than thermoplastic ones, but their mechanical properties are superior to thermoplastic materials. Still, choosing one of these materials is requires a compromise. Silicone rubber is comfortable in use due to its flexibility (soft and easily adjusts to skin), but it is also much more permeable than butyl rubber and requires additional protective hood. Butyl rubber is rigid and less comfortable but highly impermeable [72].

HD is chosen as a standard CWA agent for studying permeation and absorption processes due to its high persistence. Diffusion of sulfur mustard (HD) in butyl and nitrile rubbers was studied by Dubey et al. [73, 74], who found that HD is physically absorbed and its molecules traverse the polymer matrix via random hopping from one adsorption site to another. Low activation energies of this movement suggest a reversible nature of the sorption process. Furthermore, HD sorption and diffusion through nitrile rubber proceeds faster than through butyl rubber, and the HD solubility is higher in nitrile than in butyl rubber. The breakthrough time measurements served in determining the diffusion coefficient (3.59×10^{-11} m^2/s for butyl, and 2.17×10^{-11} m^2/s for nitrile rubber). It was shown that carbon black as a filler decreases the diffusivity of HD through butyl

---

[4] Upon increasing temperature their polymer chains are cross-linking causing the material to harden and toughen. The chemical bonds formation is irreversible. By contrast thermoplastic polymers become moldable as the temperature increases, and their chains are held together by intermolecular forces.

rubber membranes due to increased density of the membranes, but it has a negative impact on the mechanical strength of those rubbers [73].

Chosen commercial thermoplastic materials were also tested towards HD penetration by the Australian Government Department of Defence [72]. The materials selected were polyolefin based Santoprene (Advanced Elastomer Systems) and Alcryn (Advance Polymer Alloys). The polymers were blended with the following additives in order to enhance their impermeability:

- Fluorinated oil (Fluoroguard, DuPont)
- Activated carbon powder (ACTICARB PS1300, Activated Carbon Technologies)
- Fluorinated additive (Zonyl MP1100, DuPont)
- Talc clay (Talcum powder, PZ Cussons Australia Pty Ltd)

In case of talc and activated carbon the penetration resistance could be improved by extending the diffusion path due to increased tortuosity of the material (Figure 4.5), whereas fluorinated additives with low surface energy were expected to self-segregate on the surface forming continuous fluorinated layer of high chemical resistance (Figure 4.6).
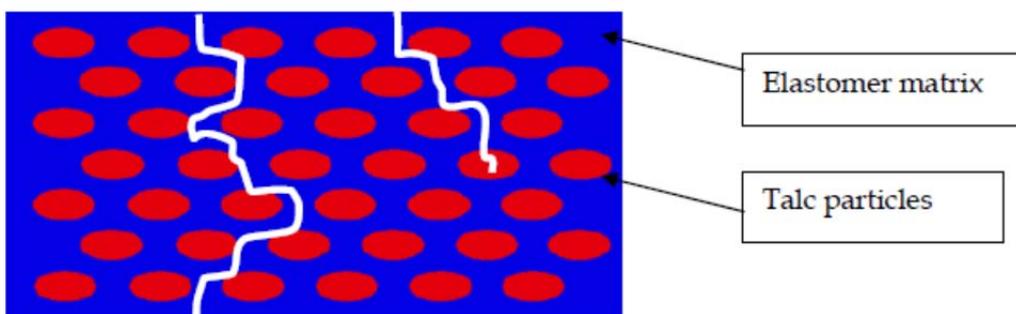
Figure 4.5 Matrix of elastomer with talc particles; white lines represent increase in penetration distance due to tortuosity (left) and adsorption on talc particles (right) [72].
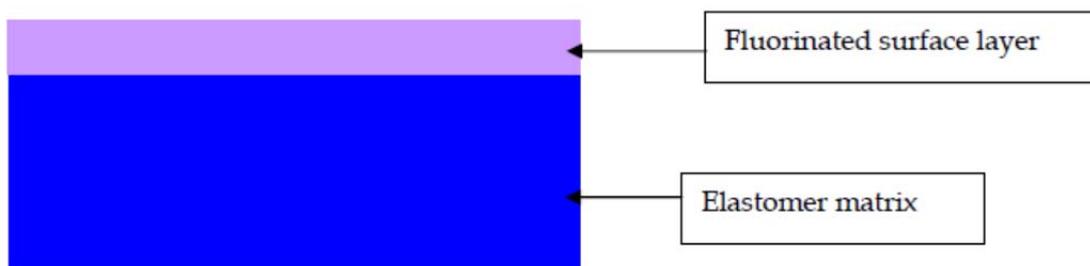

Figure 4.6 Schematic cross-section view of material with fluorinated surface layer [72].

Talc proved to be the most effective in improving the penetration resistance of the tested elastomers by 8% for 10 wt% of talc in Alcryn and 25% for same concentration of talc in

Santoprene. On the other hand, blends of elastomers and the fluorinated additives were unsuccessful, most likely due to practical difficulties in mixing and processing.

4.3 Coatings and paints

Common coatings, such as polymer-based paints can show up to 25% uptake of CWA by adsorption and permeation and can therefore be a source of long-term contamination in case of agent desorption. Chemical agent resistive coating (CARC) is a coating used to protect military equipment against CWA by limiting the CWA uptake and facilitating decontamination. CARC is a multicomponent system; apart from the top coating which is polyurethane-based, it also includes a precoating and a primer. There are different CARC systems depending on the material to be covered and the application (exterior and interior painting) (Figure 4.7).
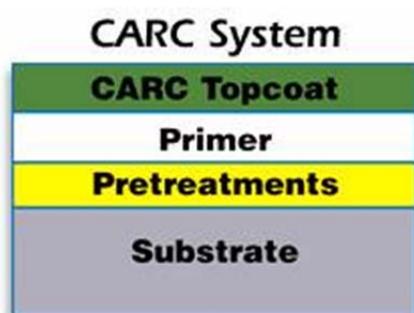
Figure 4.7   Schematic representation of CARC system cross-section [75].

In addition to chemical protection CARC systems must provide a necessary camouflage, hence different colors are available. CARC used for exterior surfaces are based on polyurethanes and in addition to chemical protection they also serve as a camouflage protection to VIS and IR means of detection. CARC for interior applications are based on epoxy paints and provide smooth, wear-resistant and easy to clean surface.

The polyurethane-based top-coat is a polymerization product between polyester and hexamethylene diisocyanate, and has -[CONH-R'-NHCOO-R-O]- repeating units [76]. The literature data available concerning the exact mechanisms of interaction and eventual uptake of CWA by CARC (Chemical agent resistive coating) are scarce, since the real-world coatings surfaces are poorly defined in terms of structure and chemical composition. However, research has been done on well-defined model surfaces such as self-assembled monolayers (SAMs) to investigate the adsorption and reactivity of CWA and their simulants. McPherson have studied the interaction of organophosphate CWA with CARC-like SAMs using several surface-sensitive methods, such as X-ray photoelectron spectroscopy (XPS), contact angle goniometry, reflection-absorption infrared spectroscopy (RAIRS), and temperature-programmed desorption (TPD) measurements [76]. In brief, the monolayers were achieved by reacting the OH-terminated alkanethiol monolayer on gold with 1,4-phenylene diisocyanate, and subsequent reaction with alcohol to yield a urethane linking group. A detailed description of CARC-like SAMS and their

synthesis can be found in [76]. No evidence of CWA uptake was found in this study, indirectly confirming the usefulness of CARC as a protective coating against organophosphate-based CWA.

Other possible concepts such as reactive coatings or strippable coatings are currently explored, yet almost all of them seem to be at relatively early development stage. The reactive coatings should react chemically with the agent yielding non-toxic products. In this respect, the diffusion of the agent throughout the coating should be fast to facilitate its transfer to the reaction sites in the entire volume of the coating. However, usually coatings are used to slow down or stop spreading of the agent through the coating (similar to CARC). Moreover, apart from typical requirements imposed to paints such as good adhesion to various surfaces and non-toxicity, the coating should meet several other criteria, such as effectiveness against wide range of CWA, durability and light weight. Especially the first prerequisite is difficult to meet, as the degradation reactions are specific. Some attempts have been made for developing the paints with catalytic or photocatalytic properties, the latter based most often on titanium dioxide TiO_2 [2]. High oxidation potential of TiO_2 towards organic molecules combined with its non-toxicity and low cost makes it particularly attractive candidate for photocatalytic applications. Nevertheless, the practical usage of such paint could be limited since it typically requires UV light to become active. Detailed information on the mechanisms of CWA degradation on oxides based on available literature data can be found in [77]. As for the catalytic systems, up to date none of them was commercialized, and further research is needed to evaluate their efficacy and versatility towards different CWA.

Finally, the strippable coating technology has recently become commercially available from AkzoNobel with the name Intergard ® 10220 [78]. It is a waterborne top coating which can be applied to CARC, however its chemical composition is unknown. According to the information available on company's website the coating absorbs "high percentage of chemical agents and holds them within the film" and in addition has infrared reflective properties. The coating is then stripped by the operator wearing an appropriate protective suit and disposed (Figure 4.8).

Figure 4.8   Intergard ® 10220, the chemical agent absorbing coating can be easily removed from the surface [78].

5   Conclusions

Despite international regulations and control CWAs still pose a threat against military forces and civilians. In particular liquid CWAs with high persistency will linger for several hours or days after CWAs involving event, causing casualties among humans and hampering the use of materiel or civilian facilities. For these reasons understanding of the phenomena occurring on the contaminated surfaces is advantageous for predicting the long-term consequences of CWAs and applying effective decontamination methods.

Chapter 2 of this report includes the general characteristics of CWA together with their persistency data and possible mechanisms of degradation in the environment, such as hydrolysis. It was shown that these mechanisms are affected, among other factors, by the chemical nature of CWAs and the contaminated surfaces. Physical and chemical properties of the exposed materials will impact wetting, spreading and uptake of liquid CWAs, which can proceed by various mechanisms, such as permeation and diffusion, mostly depending on materials porosity and structure. The general description of those mechanisms is given in Chapter 3.

Numerous studies were carried out to establish the nature of interactions between CWAs and construction materials commonly present in the urban environment. Some of the important findings in this field together with the permeability and absorption data for various materials are presented in Chapter 4. If no reaction occurs between the matrix and the CWA confined in it, the agent remains active for long periods of time and can cause casualties while desorbing. On the other hand, some of the materials have shown reactivity towards CWAs resulting in their partial or total degradation. Degradation mechanisms on the materials surfaces and in the bulk depend on many variables. In some cases a complete degradation to benign products is observed, whereas in other degradation reactions yield products of relatively high toxicity. In addition, it is generally acknowledged that the laboratory conditions often do not reflect the realistic settings; additionally some of the procedures are not standardized, which is a source of ambiguities when the data are compared. Field-scale tests or investigations on large-area surfaces exposed to different atmospheric conditions in wind tunnels would be perhaps most useful, yet such studies are expensive and pose a risk of contamination if genuine CWAs are used instead of simulants.

The results of laboratory-scale studies served to extend the knowledge on CWAs interaction with different materials and also contributed to the development of novel technologies. In particular, self-decontaminating paints, strippable coatings or slippery liquid-infused porous surfaces (SLIPS) are of interest, and implementing those technologies may be advantageous both for military forces and civilian industry. Whereas strippable coatings are technologically mature enough to be now a commercial product, the other two are under development stage. The principle of SLIPS, which is a relatively new invention and, in addition to omniphobic properties, it is promising for producing the anti-freezing coatings, has been described in Chapter 3.
Another coating currently in use is "chemical agent resistant coating" (CARC), however its exact chemical composition and interaction mechanisms with CWAs are not publicly accessible. Nevertheless, there seem to be different types of CARC coating, provided by different suppliers. The properties of CARC and its resistance towards CWAs is regulated by the NATO

documentation, however it may be also influenced by the applying techniques, ageing and other factors, which make its full characterization more complex. It would be therefore advantageous to carry out detailed investigations on real-life samples, including surfaces of vehicles, equipment and other coated surfaces currently being in use by the military forces.

References

[1]   T.-S. Wong, S. H. Kang, S. K. Y. Tang, E. J. Smythe, B. D. Hatton, A. Grinthal, *et al.*, "Bioinspired self-repairing slippery surfaces with pressure-stable omniphobicity," *Nature,* vol. 477, pp. 443-447, 2011.

[2]   G. W. Wagner, G. W. Peterson, and J. J. Mahle, "Effect of Adsorbed Water and Surface Hydroxyls on the Hydrolysis of VX, GD, and HD on Titania Materials: The Development of Self-Decontaminating Paints," *Industrial & Engineering Chemistry Research,* vol. 51, pp. 3598-3603, 2012.

[3]   S. L. Hoenig, *Compendium of Chemical Warfare Agents*. New York: Springer New York, 2007.

[4]   "Field Manual No. 3-11.9, Potential Military Chemical/ Biological Agents and Compounds," Headquarters, Department of the Army, the Navy, and the Air Force, Washington DC, 10 January 2005.

[5]   A. Malshinsky, "Chemical weapons of foreign armies and antichemical protection," DOSAAF (Volunteer Society for Cooperation with the Army, Aviation, and Fleet), Moscow CRDL Special Publication 4-23, 1957.

[6]   "Joint Publication 3-11, Operations in Chemical, Biological, Radiological, and Nuclear (CBRN) Environments," Headquarters, Department of the Army, the Navy, and the Air Force, Washington DC, 26 August 2008.

[7]   S. Franke, *Manual of Military Chemistry Volume 1. Chemistry of Chemical Warfare Agents, Deutscher Militîrverlag: Berlin (East), 1967*: Translated from German by U.S Department of Commerce, National Bureau of Standards, Institute for Applied Technology, NTIS no. AD-849 866, p. 135, 1967.

[8]   "Field Manual No. 3-5, NBC Decontamination," Headquarters, Department of the Army, Washington DC, 28 July 2000.

[9]   J. H. Blanch, B. A. Johnsen, and E. Odden, " Analysis of snow samples contamined with chemical warfare agents - part 2," *Forsvarets forskningsinstitutt, Kjeller, Norway, FFI-rapport 83/6003* 1983.

[10]   *http://www.atsdr.cdc.gov/toxprofiles/tp49-c6.pdf*.

[11]
        http://www.noblis.org/MissionAreas/nsi/BackgroundonChemicalWarfare/Chemical WarfareAgentsandChemicalWeapons/Pages/DispersalChemicalWarfareAgents.aspx

[12]   "AJP-3.8 - Doctrine for the NBC Defence of NATO Forces," NATO: North Atlantic Treaty Organization, July 2003.

[13]   A. M. Opstad and J. A. Tørnes, "Identification and quantification by GC-MS of sulfur mustard and related compounds after long time storage in sea water," Forsvarets forskningsinstitutt, Kjeller, Norway, FFI/RAPPORT-2002/03237, November 2004.

[14]   N. B. Munro, S. S. Talmage, G. D. Griffin, L. C. Waters, A. P. Watson, J. F. King, *et al.*, "The sources, fate, and toxicity of chemical warfare agent degradation products," *Environ Health Perspect,* vol. 107, pp. 933-74, Dec 1999.

[15]   M. H. Ashmore and P. C. Nathanail, "A critical evaluation of the implications for risk based land management of the environmental chemistry of Sulphur Mustard," *Environment International,* vol. 34, pp. 1192-1203, 11// 2008.

[16]   G. O. Bizzigotti, H. Castelly, A. M. Hafez, W. H. B. Smith, and M. T. Whitmire, "Parameters for Evaluation of the Fate, Transport, and Environmental Impacts of Chemical Agents in Marine Environments," *Chemical Reviews,* vol. 109, pp. 236-256, 2009/01/14 2008.

[17]   *http://www.noblis.org/MissionAreas/nsi/ChemistryofLethalChemicalWarfareAgents/Pages/ChemistryVX.aspx*.

[18]   J. Šečkutė, J. L. Menke, R. J. Emnett, E. V. Patterson, and C. J. Cramer, "Ab Initio Molecular Orbital and Density Functional Studies on the Solvolysis of Sarin and O,S-Dimethyl Methylphosphonothiolate, a VX-like Compound," *The Journal of Organic Chemistry,* vol. 70, pp. 8649-8660, 2005.

[19]   G. W. Wagner, R. J. OConnor, J. L. Edwards, and C. A. S. Brevett, "Effect of Drop Size on the Degradation of VX in Concrete," *Langmuir,* vol. 20, pp. 7146-7150, 2004.

[20]   A. H. Love, A. L. Vance, J. G. Reynolds, and M. L. Davisson, "Investigating the affinities and persistence of VX nerve agent in environmental matrices," *Chemosphere,* vol. 57, pp. 1257-1264, 2004.

[21]   J. A. Cragan, M. C. Ward, and C. B. Mueller, "Modeling the pH dependent hydrolysis of VX for aqueous releases," *Journal of Hazardous Materials,* vol. 170, pp. 72-78, 2009.

[22]   W. E. Steiner, S. J. Klopsch, W. A. English, B. H. Clowers, and H. H. Hill, "Detection of a chemical warfare agent simulant in various aerosol matrixes by ion mobility time-of-flight mass spectrometry," *Analytical chemistry,* vol. 77, pp. 4792-4799, 2005.

[23]   P. W. Atkins, *Physical Chemistry*. Oxford Melbourne Tokyo: Oxfor University Press, 1998.

[24]   W. A. Zisman, "Relation of the Equilibrium Contact Angle to Liquid and Solid Constitution," in *Contact Angle, Wettability, and Adhesion*. vol. 43, ed: AMERICAN CHEMICAL SOCIETY, 1964, pp. 1-51.

[25]   R. Shuttleworth, "The Surface Tension of Solids," *Proceedings of the Physical Society. Section A,* vol. 63, p. 444, 1950.

[26]   L. Makkonen, "Misinterpretation of the Shuttleworth equation," *Scripta Materialia,* vol. 66, pp. 627-629, 2012.

[27]   J. Ledgard, *A Laboratory History of Chemical Warfare Agents*. USA, 2006.

[28]   *http://en.wikipedia.org/wiki/File:Paper_Clip_Surface_Tension_1.jpg*.

[29]   I. Gentle and G. Barnes, *Interfacial science : an introduction*. Oxford ; New York: Oxford University Press, 2005.

[30]   *http://www.dsm.com/en_US/html/dep/adhesive_bonding.htm*.

[31]   R. N. Wenzel, "Resistance of solid surfaces to wetting by water," *Industrial & Engineering Chemistry,* vol. 28, pp. 988-994, 1936.

[32]   A. B. D. Cassie and S. Baxter, "Wettability of porous surfaces," *Transactions of the Faraday Society,* vol. 40, pp. 546-551, 1944.

[33]   E. Stratakis, A. Ranella, and C. Fotakis, "Biomimetic micro/nanostructured functional surfaces for microfluidic and tissue engineering applications," *Biomicrofluidics,* vol. 5, 2011.

[34]   I. F. W. Kuo, C. D. Grant, R. H. Gee, S. C. Chinn, and A. H. Love, "Determination of the Surface Effects on Sarin Degradation," *The Journal of Physical Chemistry C,* vol. 116, pp. 9631-9635, 2012.

[35]
         https://www.fbo.gov/index?s=opportunity&mode=form&tab=core&id=871d16a390520 ab3bbb392316ba9d294.

[36]   B. Petkovic, "Deposition of Droplets onto Solid Objects in Aerosol Flow," Master of Applied Science, Faculty of Graduate Studies, Chemical and Biological Engineering, University of British Columbia, Vancouver, 2010.

[37]   A. Agrawal. (2005, 02.11.2012). *Surface Tension of Polymers*. Available: http://web.mit.edu/nnf/education/wettability/summerreading-2005short.pdf

[38]   M. Nosonovsky, "Materials science: Slippery when wetted," *Nature,* vol. 477, pp. 412-413, 2011.

[39]   P. Kim, T.-S. Wong, J. Alvarenga, M. J. Kreder, W. E. Adorno-Martinez, and J. Aizenberg, "Liquid-Infused Nanostructured Surfaces with Extreme Anti-Ice and Anti-Frost Performance," *ACS Nano,* vol. 6, pp. 6569-6577, 2012.

[40]   X. Zhang and O. A. Basaran, "Dynamic Surface Tension Effects in Impact of a Drop with a Solid Surface," *Journal of Colloid and Interface Science,* vol. 187, pp. 166-178, 1997.

[41]   M.-J. Wang, F.-H. Lin, J. Y. Ong, and S.-Y. Lin, "Dynamic behaviors of droplet impact and spreading—Water on glass and paraffin," *Colloids and Surfaces A: Physicochemical and Engineering Aspects,* vol. 339, pp. 224-231, 2009.

[42]   Š. Šikalo and E. N. Ganić, "Phenomena of droplet–surface interactions," *Experimental Thermal and Fluid Science,* vol. 31, pp. 97-110, 2006.

[43]   Š. Šikalo, M. Marengo, C. Tropea, and E. N. Ganić, "Analysis of impact of droplets on horizontal surfaces," *Experimental Thermal and Fluid Science,* vol. 25, pp. 503-510, 2002.

[44]   D. Comeau, K. LaTourette, and J. Pate. December 6, 2007). To splash or not to splash . . . The efect of Weber number and spread factor of a water droplet impinging on a super-hydrophobic substrate. *2007*. Available: http://math.arizona.edu/~dcomeau/research/CLPpresentation.pdf

[45]   B. Durickovic and K. Varland. (2005, Between Bouncing and Splashing: Water Drops on a Solid Surface. Available: http://pub.bojand.org/bounce.pdf

[46]   B. Markicevic, H. Li, Y. Sikorski, A. R. Zand, M. Sanders, and H. K. Navaz, "Infiltration time and imprint shape of a sessile droplet imbibing porous medium," *Journal of Colloid and Interface Science,* vol. 336, pp. 698-706, 2009.

[47]   N. C. Reis Jr, R. F. Griffiths, and J. M. Santos, "Parametric study of liquid droplets impinging on porous surfaces," *Applied Mathematical Modelling,* vol. 32, pp. 341-361, 2008.

[48]   B. Markicevic and H. K. Navaz, "Primary and Secondary Infiltration of Wetting Liquid Sessile Droplet into Porous Medium," *Transport in Porous Media,* vol. 85, pp. 953-974, 2010.

[49]   B. Markicevic, T. G. D'Onofrio, and H. K. Navaz, "On spread extent of sessile droplet into porous medium: Numerical solution and comparisons with experiments," *Physics of Fluids,* vol. 22, pp. 012103-12, 2010.

[50]   H. K. Navaz, B. Markicevic, A. R. Zand, Y. Sikorski, E. Chan, M. Sanders*, et al.*, "Sessile droplet spread into porous substrates—Determination of capillary pressure using a continuum approach," *Journal of Colloid and Interface Science,* vol. 325, pp. 440-446, 2008.

[51]   N. C. Reis Jr, R. F. Griffiths, and J. M. Santos, "Numerical simulation of the impact of liquid droplets on porous surfaces," *Journal of Computational Physics,* vol. 198, pp. 747-770, 2004.

[52]   S. H. Hong, K. B. Sumpter, W. J. Shuely, and R. G. Nickol, "Evaporation of HD droplets from nonporous, inert surfaces in TGA microbalance wind tunnels," AberdeenSeptember 2008.

[53]   R. F. Griffiths and I. D. Roberts, "Droplet evaporation from porous surfaces; model validation from field and wind tunnel experiments for sand and concrete," *Atmospheric Environment,* vol. 33, pp. 3531-3549, 1999.

[54]   O. Busmundrud, " Fordamping fra overflater og dråper," Forsvarets forskningsinstitutt, Kjeller, Norway, FFI/RAPPORT-2005/03538, November 20052005.

[55]   T. Vik and B. A. P. Reif, "Preliminary assessment of the vertical release of liquefied chlorine inside a depression," Forsvarets forskningsinstitutt, Kjeller, Norway, FFI-rapport 2009/01251, August 20112011.

[56]   T. Vik and B. A. P. Reif, "Modeling the evaporation from a thin liquid surface beneath a turbulent boundary layer," Forsvarets forskningsinstitutt, Kjeller, Norway, FFI-rapport 2010/00254, October 20102010.

[57]   T. Vik and B. A. P. Reif, "Implementation of a new and improved evaporation model in Fluent," Forsvarets forskningsinstitutt, Kjeller, Norway, FFI-rapport 2011/00116, January 20112011.

[58]   S. N. Westin, S. Winter, E. Karlsson, A. Hin, and F. Oeseburg, "On modeling of the evaporation of chemical warfare agents on the ground," *Journal of Hazardous Materials,* vol. 63, pp. 5-24, 1998.

[59]   I. C. MacGregor, J. V. Rogers, D. V. Kenny, T. Hayes, M. L. Taylor, M. G. Nishioka*, et al.*, "Persistence of Toxic Industrial Chemicals and Chemical Warfare Agents on

Buildng Materials Under Conventional Environmental Conditions, EPA/600/R-08/075, July 2008," U.S. Environmental Protection Agency.

[60]   A. Heller. (2010) Responding to a Terrorist Attack. *Science & Technology Review* [review]. 6. Available: https://str.llnl.gov/Mar10/koester.html

[61]   "Chemical, Biological, Radiological and Nuclear (CBRN) Contamination Survivability Factors in the Design, Testing and Acceptance of Military Equipment," NATO ARMY ARMAMENTS GROUP (NAAG) NATO/PfP AEP-7 Ed.5, 2012.

[62]   *http://matse1.matse.illinois.edu/concrete/prin.html*

[63]   H. Tang, Z. Cheng, M. Xu, S. Huang, and L. Zhou, "A preliminary study on sorption, diffusion and degradation of mustard (HD) in cement," *Journal of Hazardous Materials,* vol. 128, pp. 227-232, 2006.

[64]   C. A. S. Brevett, K. B. Sumpter, G. W. Wagner, and J. S. Rice, "Degradation of the blister agent sulfur mustard, bis(2-chloroethyl) sulfide, on concrete," *Journal of Hazardous Materials,* vol. 140, pp. 353-360, 2007.

[65]   C. A. S. Brevett, K. B. Sumpter, and R. G. Nickol, "Kinetics of the degradation of sulfur mustard on ambient and moist concrete," *Journal of Hazardous Materials,* vol. 162, pp. 281-291, 2009.

[66]   C. A. S. Brevett and K. B. Sumpter, "Sulfur Mustard Degradation on Ambient and Moist Concrete," Edgewood Chemical Biological Center US Army Research, Development and Engineering Command ECBC-TR-641, 08.2008 2008.

[67]   D. M. Mizrahi, M. Goldvaser, and I. Columbus, "Long-Term Evaluation of the Fate of Sulfur Mustard on Dry and Humid Soils, Asphalt, and Concrete," *Environmental Science & Technology,* vol. 45, pp. 3466-3472, 2011.

[68]   G. S. Groenewold, A. D. Appelhans, G. L. Gresham, J. E. Olson, M. Jeffery, and M. Weibel, "Characterization of VX on concrete using ion trap secondary ionization mass spectrometry," *Journal of the American Society for Mass Spectrometry,* vol. 11, pp. 69-77, 2000.

[69]   G. S. Groenewold, J. M. Williams, A. D. Appelhans, G. L. Gresham, J. E. Olson, M. T. Jeffery*, et al.*, "Hydrolysis of VX on Concrete: Rate of Degradation by Direct Surface Interrogation Using an Ion Trap Secondary Ion Mass Spectrometer," *Environmental Science & Technology,* vol. 36, pp. 4790-4794, 2002.

[70]   G. W. Wagner, R. J. O'Connor, and L. R. Procell, "Does Concrete Self-Decontaminate VX," 2003.

[71]   G. W. Wagner, R. J. O'Connor, J. L. Edwards, and C. A. Brevett, "Degradation And Decontamination of VX in Concrete," 2004.

[72]   P. Miller, "Sulfur Mustard Penetration of Thermoplastic Elastomers," Defence Science and Technology Organisation (Australia). Human Protection and Performance Division2008.

[73]   V. Dubey, N. B. Rao, S. N. Maiti, and A. K. Gupta, "Sorption of sulfur mustard and its oxygen analog in black and nonblack-filled butyl rubber membranes," *Journal of Applied Polymer Science,* vol. 69, pp. 503-511, 1998.

[74]   V. Dubey, A. K. Gupta, and S. N. Maiti, "Mechanism of the diffusion of sulfur mustard, a chemical warfare agent, in butyl and nitrile rubbers," *Journal of Polymer Science Part B: Polymer Physics,* vol. 40, pp. 1821-1827, 2002.

[75]   *http://www.inetres.com/gp/military/cv/carc.html*.

[76]   M. K. McPherson, "The Reactivity of Chemical Warfare Agent Simulants on Carbamate Functionalized Monolayers and Ordered Silsesquioxane Films," PhD PhD dissertation Chemistry, Virginia Polytechnic Institute and State University, Blacksburg, Virginia, 2005.

[77]   K. Mo and S. R. Sellevåg, "Adsorption and degradation of chemical warfare agents on oxides, FFI-rapport 2010/01775," Norwegian Defence Research Establishment (FFI)2010.

[78]   *http://www.anac.com/Brochures/AkzoNobel_Intergard_10000.pdf*.